Discussion on Electric Power Supply Systems for All Electric Aircraft

HENDRIK SCHEFER[ID]**[1], LEON FAUTH**[ID]**[2], (Member, IEEE), TOBIAS H. KOPP**[ID]**[3],
REGINE MALLWITZ[1]**, (Member, IEEE), JENS FRIEBE**[ID]**[2], (Member, IEEE),
AND MICHAEL KURRAT[3]**, (Member, IEEE)**
[1]Institute for Electrical Machines, Traction and Drives, Technische Universität Braunschweig, 38106 Braunschweig, Germany
[2]Institute for Drive Systems and Power Electronics, Leibniz Universität Hannover, 30167 Hannover, Germany
[3]Institut für Hochspannungstechnik und Elektrische Energieanlagen - elenia, Technische Universität Braunschweig, 38106 Braunschweig, Germany

Corresponding author: Regine Mallwitz (r.mallwitz@tu-braunschweig.de)

ABSTRACT The electric power supply system is one of the most important research areas within sustainable and energy-efficient aviation for more- and especially all electric aircraft. This paper discusses the history in electrification, current trends with a broad overview of research activities, state of the art of electrification and an initial proposal for a short-range aircraft. It gives an overview of the mission profile, electrical sources, approaches for the electrical distribution system and the required electrical loads. Current research aspects and questions are discussed, including voltage levels, semiconductor technology, topologies and reliability. Because of the importance for safety possible circuit breakers for the proposed concept are also presented and compared, leading to a initial proposal. Additionally, a very broad review of literature and a state of the art discussion of the wiring harness is given, showing that this topic comes with a high number of aspects and requirements. Finally, the conclusion sums up the most important results and gives an outlook on important future research topics.

INDEX TERMS Aviation, aerospace electronics, MEA, AEA, electric power supply systems, dc-dc power converters, power semiconductor devices, wide bandgap semiconductors, high voltage direct current (HVDC), circuit breaker, hybrid circuit breaker.

AEA	All Electric Aircraft	**EMA**	Electro-Mechanical Actuators
ALFCS	Active Laminar Flow Control System	**EMC**	Electromagnetic Compatibility
ANPC	Active Neutral Point Clamped	**EMI**	Electromagnetic Interference
APES	Auxiliary Power Electronics Switch	**EPS**	Expand Phase Shift Modulation
APU	Auxiliary Power Unit	**eVTOL**	All-Electrical Vertical Take-Off and Landing
ATAG	Air Transport Action Group		
BMU	German Federal Ministry for the Environment, Nature Conservation and Nuclear Safety	**EXT-PWR**	External Power Supply
		FAA	Federal Aviation Administration
bti	bias temperature instability	**FIT**	Failure in Time
CB	Circuit Breaker	**GaN**	Gallium Nitride
CSCE	Critical Short-Circuit Energy	**GPU**	Ground Power Unit
DAB	Dual Active Bridge	**HEMT**	High Electron Mobility Transistor
DCB	Direct Copper Bonding	**HVDC**	High Voltage DC
EPAS	European Plan for Aviation Safety	**IATA**	International Air Transport Association
ECS	Environmental Control System	**IGBT**	Insulated Gate Bipolar Transistors
EHA	Electro-Hydraulic Actuators	**JEDEC**	JEDEC Solid State Technology Association
		MEA	More Electric Aircraft
		MFFC	Multifunctional Fuel Cell

MMC	Modular Multilevel Converter
MOSFET	Metal Oxide Field-Effect Transistors
MPES	Main Power Electronic Switch
MS	Mechanical Switch
pax	Passengers
PD	Partial Discharge
PE	Power Electronic
PoL	Point of Load
RAT	Ram Air Turbine
SBD	Shottky Barrier Diode
SCC	Switched Capacitor Converter
SCWT	Short-Circuit Withstand Time
SEB	Single Event Burnout
SEE	Single Event Effect
SEGR	Single Event Gate Rupture
Si	Silicon
SiC	Silicon Carbide
SoC	State of Charge
SPS	Single Phase Shift Modulation
SSCB	Solid State Circuit Breaker
SSPC	Solid State Power Controller
STARC-ABL	Single-aisle Turboelectric AiRCraft with Aft Boundary Layer propulsion
SUGAR	Subsonic Ultra Green Aircraft Research
TID	Total Ionizing Dose
TPS	Triple Phase Shift Modulation
VFSG	Variable Frequency Starter Generator
WIPS	Wing Ice Protection System
ZVS	Zero Voltage Switching

I. INTRODUCTION

Two key drivers for electrifying air transportation can be identified: First, pollution as a result of the ever-increasing number of flights needs to be limited, if current climate goals are to be reached. Here, especially the high amount of CO_2 emission by conventional jet turbines needs to be reduced [1]. Secondly, the availability of currently used jet fuel refined from oil is limited - therefore, new driving concepts or fuels need to be investigated. Additionally, prices are expected to increase in the long term [2], which will result in a lower profit margin, as fuel prices hold a large share in overall aircraft operation costs [3]. As a result, there is a trend towards a more ecological alternative, which will ultimately mean a strong electrification of aircraft. The first step is the so-called More Electric Aircraft (MEA), which will increase overall efficiency by replacing conventional solutions with electrically driven alternatives [4], [5]. In the next step, in the All Electric Aircraft (AEA) the thrust components will also be replaced with electric systems, prospectively in a series hybrid concept for medium- to long-range applications. To make this concept feasible, progress in a multitude of areas is needed. As batteries are a possible energy source for future AEA, a high overall efficiency is mandatory. Therefore, research in improved aerodynamics is necessary. For weight savings, novel fuselage and wing materials have to

be considered. For the electrical systems, high efficiency electrical drives as well as high power density energy sources are needed [6]. Interconnecting the sources as well as the loads, which includes beside the motors additionally the Wing Ice Protection System (WIPS), the Environmental Control System (ECS), the control flaps, avionics, hotel and galley loads and more, requires a high efficiency energy distribution system. This electrical grid can therefore be seen as key driver for energy-efficient aviation. It enables novel approaches for aircraft energy supply from source to load with new grid structures and distributed energy generation systems. Electrical sources can be high energy density batteries and fuel cells, being already a wide area of current research [7]–[9]. Also the voltage level and frequency for the electrical grid need to be considered, as they directly relate to the system topology and overall weight. For reducing the current and therefore the diameter of the wiring harness, High Voltage DC (HVDC) grids are proposed [10]. While the here described voltages, although described as HVDC, do not exceed 540 V($\pm$270 V), even higher DC voltages up to 3 kV($\pm$1.5 kV) will be examined in this publication. Based on this, an energy supply system for an AEA consisting of DC/DC converters, wiring harness and circuit breakers will be proposed. This system will be sized for the use in a typical regional commuter aircraft with less than 100 Passengers (pax). Challenges with regard to energy generation, conversion and distribution will be highlighted, with a focus on the power electronics switches and topologies, high power circuit breakers and wiring harness reliability. Especially challenges coming from the application in an aircraft environment, which is characterized by low pressure, harsh temperatures and radiation, are identified. The feasible solutions are based on a high voltage distribution grid, enabled by novel wide bandgap semiconductor devices with high breakdown voltage as well as special topologies for high voltages and high currents. For circuit breakers, new hybrid structures are discussed. Section II and III give an overview of the current state of the art regarding the air transportation system. Section IV gives details on current MEAs. In Section V, advantages and disadvantages of a high voltage distribution system will be shown, followed by an initial proposal for a high voltage grid for an AEA in Section VI. Power electronics devices based on Silicon Carbide (SiC) and Gallium Nitride (GaN) and their special use in an aircraft environment are discussed in Section VII. Section VIII introduces different topologies for high voltage and high current circuit breakers, Section IX discusses challenges for a high voltage wiring harness in an aircraft environment.

II. TRANSFORMATION TOWARDS SUSTAINABLE AIR TRANSPORT

The transformation of society towards a more sustainable use of resources is the focus of a large number of research projects. A growing world population, decreasing resources, increasing demands on the quality of life, and changing living conditions represent significant challenges for the present and future generations on earth. Especially the environmental

conditions are fundamental for the existence of our society. An essential factor for the sustainable development of humanity is mobility with the help of individual and public transport.

A. ENVIRONMENTAL IMPACT

In Germany, the transportation sector was responsible for 18 % of CO_2 equivalents in 2016. In contrast to other sectors such as energy, industry, agriculture, waste management, and private households, the CO_2 rose by 3 % in 2017 compared to the reference year 1990. According to the German Federal Ministry for the Environment, Nature Conservation and Nuclear Safety (BMU), 1.4 % of emissions from the transport sector are attributable to national flights [11, page: 39] [12].

Civil aviation within Europe is responsible for 13.2 % of CO_2 emissions in the transport sector [13]. The European Aviation Environmental Report 2019 shows a relative increase of 16 % in CO_2 emissions compared to the reference year of 2005 to 2017. A further increase of 42 % is expected according to current models. Nitrogen oxide emissions also show drastic increases. Besides, the report shows only a positive development in noise reduction.

Worldwide, the impact of air traffic on the environment is estimated to be 2 % of the anthropogenic carbon dioxides [14].

B. MARKET PROSPECTS

The International Air Transport Association (IATA) predicts that passenger numbers will double from 2016 to 2030 under liberal market conditions and political stimulus. Asia is expected to show high growth rates [15]. Currently, only 10 % of the world population has access to air travel [16].

Another important criterion is the price development of kerosene. According to a worst-case estimate, the price of crude oil could double by 2050. The kerosene price is directly linked to the price of crude oil [17, page: 16]. CO_2 taxes related to passengers and per 100 km are under discussion.

C. POLICY INSTRUMENTS

The Paris Agreement is an essential target for global climate protection and the preservation of livelihoods. The agreement aims at a global warming of below two degrees Celsius compared to pre-industrial age [18]. The European Flightpath also addresses ambitious environmental protection goals for civil aviation. By 2050, the technologies are expected to reduce CO_2 emissions by 75 % per passenger kilometer, nitrogen oxide emissions by 90 %, and noise emissions by 65 %. The reference is a new type of aircraft from the year 2000. These specifications support the Air Transport Action Group (ATAG) target [1, page: 15]. Further objectives of the Flightpath are

- emission-free taxiing,
- air vehicles have to be designed and manufactured so as to be recyclable,

- Europe is established as a center of excellence for sustainable alternative fuels, including those for aviation, based on a robust European energy policy,
- Europe is at the forefront of atmospheric research and takes the lead in the formulation of a prioritized environmental action plan and establishment of global environmental standards.

Noise and nitrogen oxide reduction addresses urban areas in particular. Many European airports have a ban on night flights.

D. RESEARCH APPROACHES

Based on the goals mentioned above, a series of research projects can be developed, which will lead to an evaluation of air traffic systems, flight physics, vehicle systems, energy storage, and conversion. Sustainable air transport requires a low carbon footprint, low noise footprint, high operational safety, and high reliability at low cost under the high complexity of the entire aviation system. Known vital parameters are the reduction of aerodynamic drag by new aerodynamic concepts, reduction of structural masses by new materials, and integration of propulsion systems.

Synthetic fuel can be used for CO_2-neutral air traffic. A further optimization is the electrification of the aircraft, which could lead to very low-noise and low-emission air traffic. For this purpose, power densities of electrical components must be increased, energy densities of electrical storage media must be improved, and sustainable generation and transport of electrical energy must be achieved.

The next section deals in detail with realized aircraft concepts, so-called MEAs, and well-known research projects on platforms of hybrid aircraft. It derives the trend of electrification without referring to the aircraft category.

III. TREND OF ELECTRIFICATION IN AIRCRAFT APPLICATIONS

Fig. 1 shows the predicted development of electrification in commercial aviation. In this case, the electrical power requirement is plotted logarithmically over the year. There are numerous other research projects, such as All-Electrical Vertical Take-Off and Landing (eVTOL) or small regional electrified aircraft (e.g.: Zunum Aero), which are not included in this diagram.

For the listed commercial aircraft and research projects, the ratio of electrification is given. The ratio $\frac{P_{el}}{P_{th}}$ of the electrical power to the maximum thrust power in take-off is put into relation. The thrust power is estimated here and is not a standard parameter in aviation industry.

A. AIRBUS A380

The Airbus A380 can be classified among the MEA, it was commissioned in 2007 and had a maximum capacity of 853 seats (typical seating 4-class: 550 seats). The aircraft has a cruising speed of 0.89 Mach and a range of 14, 800 km (8, 000 NM) [19]. Hydraulic components are partly electrified, such as flight control systems. The increased electrical
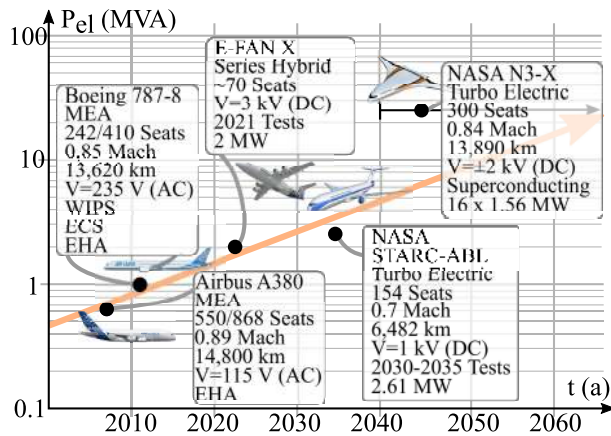
FIGURE 1. Trend of electrification in aviation application.

power requirement is provided by four generators of the main engines (600 kVA in total, $\frac{P_{el}}{P_{th}} < 0.2\,\%$, excluding the Auxiliary Power Unit (APU)) with an alternating voltage of 115 V [20, page: 57]. 75 g CO_2 per passenger kilometer are achieved by using expanded materials and reducing the structural mass. This airplane reduces noise emissions by 50 % at take-off and three to four times less noise at landing compared to its nearest competitor. The engines reduce noise emissions with a combined wing and landing gear design [19].

B. BOEING 787
A further MEA is the Boeing 787-8 Dreamliner, launched in 2011 with a maximum of 410 pax (typical 242 pax). In flight operation, a cruising speed of 0.85 Mach, and a range of 13, 620 km (7, 354 NM) is achieved [21]. In this type of aircraft, a large number of pneumatic and hydraulic systems were replaced by electric ones. Power electronics and electrical machines with compressors replace huge pneumatic loads, such as the WIPS and the ECS. Due to the high electrical power requirement, an on-board grid with an alternating voltage of 235 V was implemented. The four generators of the two main engines generate a total electrical power of 1 MVA (without APU, $\frac{P_{el}}{P_{th}} < 1.5\,\%$) [20, page: 57]. Composite materials and an optimized aircraft structure are also used. These technologies enable noise emissions to be reduced by 60 % and fuel consumption by 20 % [21].

C. E-FAN X
E-FAN X is a project initially led by Airbus, Rolls Royce and Siemens. The first test flights are expected in 2021. The BAe 146 is powered by four engines. One propulsion unit is powered by a 2 MW ($\frac{P_{el}}{P_{th}} \approx 25\,\%$) electric motor and connected to the 3 kV on-board power supply via an inverter. It is a serial hybrid system; a built-in turbine drives a generator in the fuselage [22], [23, page: 10]. The platform is designed to explore challenges such as thermal management, altitude, and dynamic effects in high-performance electrical propulsion systems while maintaining high reliability and safety [24].

D. NASA STARC-ABL
NASA project Single-aisle Turboelectric AiRCraft with Aft Boundary Layer propulsion (STARC-ABL) combines several experiences from projects such as Subsonic Ultra Green Aircraft Research (SUGAR) and N3X. For the first tests, the availability of the Turbofan N + 3 technology is essential. The technology is expected to be available in the time frame 2030 to 2035. With a cruising speed of 0.7 Mach, a range of 6, 482 km (3, 500 NM), and 154 pax, the aircraft belongs to the medium range [25, pages: 2-3]. It is a parallel hybrid, the engines below the wings generate thrust and electrical power. Thus, each engine generates electrical power of roughly 1.5 MW and is connected via an inverter to a 1 kV DC on-board power supply. The DC system is connected to a boundary layer ingesting tail-one thruster. The all-electric drive has a power of roughly 2.61 MW ($\frac{P_{el}}{P_{th}} \approx 30\,\%$) and generates thrust. Due to the installation situation, as a boundary layer ingesting tail-one thruster, the engines can be optimized under the wings. The combination of smaller engines on the wings and the boundary layer ingesting tail-one thruster reduces the aerodynamic drag [26, pages: 2-3].

E. NASA N3-X
Another NASA project, N3-X, is strongly oriented towards the NASA Future Aircraft Goals N + 3. Another important milestone will be the availability of turbofan technology, and a maiden flight would be possible from 2040 [27, page: 3]. The aircraft has a cruising speed of 0.84 Mach, a distance of 13, 890 km (7, 500 NM), and carries 300 pax [28, page: 9]. Studies show that the best possible weight reduction can be achieved using superconductivity and a DC on-board network of ±2 kV [29, page: 197]. Besides, two generators with 6.5 MW each are operated per wing. Sixteen distributed electric drive systems provide the thrust as After Fan Technology. The target is a nominal total electrical output 25 MW ($\frac{P_{el}}{P_{th}} \approx 80\,\%$) [29, page: 135]. With the help of the Hybrid Wing Body with Nacelle (HWB), the aerodynamic drag is reduced. The improvements will reduce fuel consumption by 60 % and reduce nitrogen oxide emissions by 80 % during take-off and landing [30, pages: 1-2]. A noise-optimized variant has an estimated noise reduction of 64EPNdB under flight noise standard "Chapter 4 standard cumulative margin noise reduction" [30, pages:19-20].

F. ESTIMATION OF THE AVAILABLE ELECTRICAL POWER
The orange arrow in Fig. 1 shows the trend towards electrification. MEA and Hybrid-electric Aircraft such as E-FAN X and NASA STARC-ABL illustrate the trends. According to these estimations, 10 MW of electrical power could be implementable in an aircraft in 2050.

A good system concept and HVDC transmission are required to enable this vision. For this approach, great efforts are required in search of electrical systems for aviation purposes. In 2050, it seems feasible to operate AEA in the short and medium range.

For the NASA N3-X concept, a major technological leap must follow, involving the use of a combined HVDC transmission with superconductivity. In addition, the power densities of power electronics and electrical machines must increase drastically, achieved for example by using new materials and superconductivity. These approaches require high investment costs in these research projects.

The following section presents the state of the art by a large commercial MEA.

IV. STATE OF ART: ELECTRICAL ARCHITECTURE OF A LARGE COMMERCIAL MORE ELECTRIC AIRCRAFT

Two well-known commercial concepts of a MEA could be identified from Section II. The aircraft aims at saving fuel in order to minimize airline costs and carbon dioxide emissions. Another goal is to reduce aircraft noise. MEAs are the first steps towards sustainable commercial air traffic, as defined by the overall social goals.

In the following section, the aircraft concept is presented from the point of view of the electrical components, although a great deal of engineering effort is also involved in optimizing the structural mass, the aerodynamic concept, and other disciplines. It is shown how the on-board grid has changed in comparison to a typical aircraft and the influence involved on the overall system. The secondary power systems in an aircraft, such as hydraulics, pneumatics, mechanics, and electricity, have an influence of approximately 5 % on the total fuel consumption. They are essential for safe flight operations and passenger comfort [23, page: 1].

Fig. 2 shows the on-board grid of a large commercial aircraft, based on the Boeing 787, and is supposed to illustrate the ongoing development. Individual components are represented schematically in the figure. In the presented aircraft, many pneumatic and some parts of hydraulic components have been replaced by electrical ones. A better condition monitoring and controllability characterizes electrical components in comparison to bleed-air based systems so that consumption-oriented energy is available. Besides, individual subsystems can be switched off easily in the event of a fault [31, page: 8].

The MEA concept uses the Boeing 787's no-bleed system architecture. By replacing the bleed air, better fuel efficiency is achieved due to better use of secondary energy, maintenance costs are reduced due to the exchange of pneumatic systems, and higher reliability is obtained with modern power electronics and component reduction [32, page: 6]. A conventional aircraft has a bleed-air system with roughly 1.2 MW [33, page: 2]. This method saves approx. 3 % of the fuel [32, page: 6]. Compared to conventional architectures, weight and lifecycle costs are reduced.

A. MAIN ENGINE AND GENERATOR

In traditional aircraft, the bleed air is removed from the turbine, resulting in inefficient utilization. In contrast, a modern commercial aircraft replaces the bleed-air extraction system with larger Variable Frequency Starter Generators (VFSGs).

The replacement requires a higher electrical system performance [33, pages: 2-3]. Fig. 2 shows two VFSGs per turbine with an output of 250 kVA each. Thus, an electrical system power of 1 MVA is available [32, page: 9].

In traditional aircraft, the turbine is started via the pneumatics (so-called Main Engine Start); in MEA, this is achieved electrically via starter converters. The electrical power is provided by the APU, the other turbine or the External Power Supply (EXT-PWR). The jet engine can be started via the APU or the other already started jet turbine or a ground vehicle [32, page: 9-11].

Another difference to the typical aircraft is the variable electrical frequency, which is within the range of 360 to 800 Hz in the represented MEA. In previous aircraft, an Integrated Drive Generator ($f = 400$ Hz) is used, which consists of a generator and a Constant Speed Drive. However, today's three-phase VFSG uses a fixed ratio gear connected to the high-pressure turbine stage. No power electronics are needed for this approach. Permanent magnet synchronous generators can be an alternative to achieve a higher power density of 8 kVA/kg (currently 3.3 kVA/kg, VFSG) [23, page: 652]. The proximity of the turbine to the electrical machine requires proper thermal management. A further increase in the electrical system performance lacks a multiple spool concept (currently: high-pressure stage of main engine is used) [23, page: 653].

B. AUXILIARY POWER UNIT

The APU turbine stage at the rear does not contain any pneumatics. The APU also uses a VFSG and is less complex than its predecessor. In typical aircraft, the APU has a pneumatic system for starting the main engines [32, page: 11] [20, page: 57].

Efforts are being made to replace the APU with a Multifunctional Fuel Cell (MFFC) system. The system generates electrical energy and heat. In addition, water is available to the aircraft through a treatment process. Another possibility of the use of MFFC is the generation of nitrogen. Nitrogen can be used as an inert gas to prevent the ignition of the fuel in the tank [34, page: 20-28] [35, pages: 5] [36, pages: 1-3].

C. ELECTRICAL POWER SUPPLY

Because the electrical system power has increased dramatically by replacing the bleed air, the effective alternating voltage of the three-phase system is increased to 235 V (typically 115 V). Fig. 2 shows a distributed redundant electrical power system, which is centralized in a typical aircraft. Furthermore, for compatibility reasons, the voltage level 115 V AC and 28 V DC is used, since many components are designed for this voltage level and many airports provide this external power supply. The DC voltage of ± 270 V is mostly generated by passive three-phase bridge rectifiers (so-called Auto Transformer Rectifier) and is used to supply components with high electrical power, such as the compressors for the ECS. [32, page: 9].
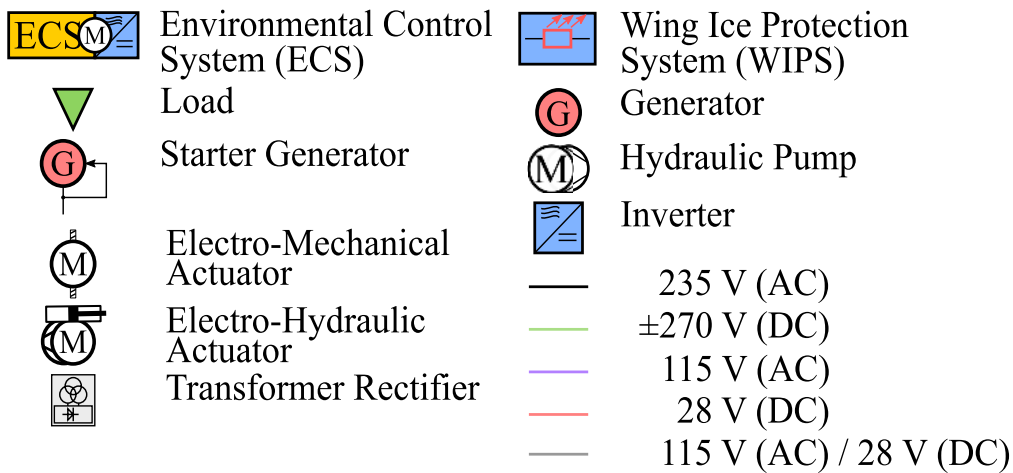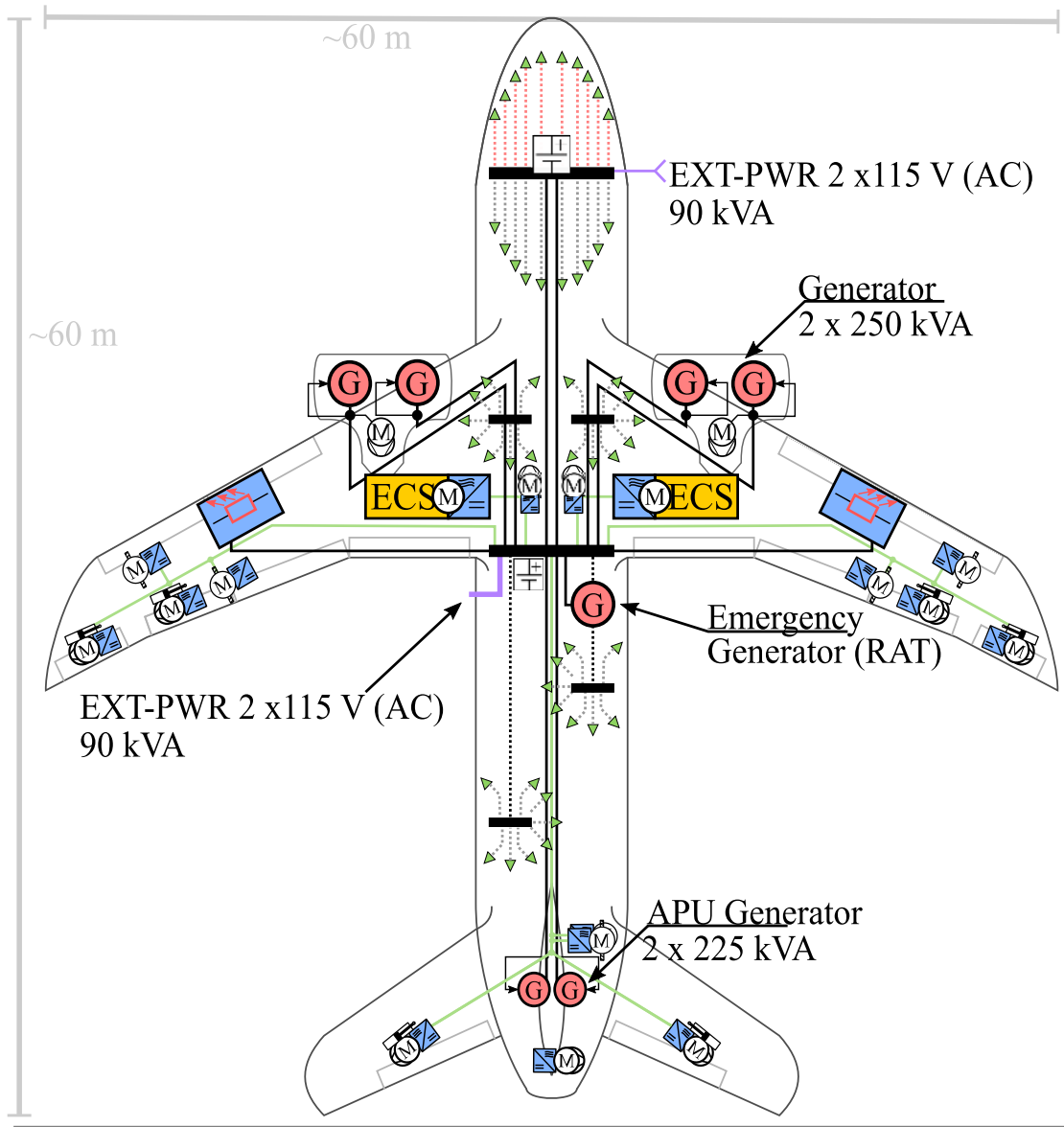
FIGURE 2. Electric schematic of MEA.

One research effort for MEA is to increase the voltage of the electrical power supply system to 540 V DC. The standards, such as MIL-STD-704F, have to be adapted. Arcing represents a major risk under such harsh environmental conditions.

A further challenge is the increasing demand for power and the associated power generation. Low-speed turbine stages could be used. Wide bandgap semiconductors represent an alternative to silicon. The wider fundamental wave of the electrical machine at low pressure stage and the increased on-board voltage pose a challenge for conventional semiconductor materials [23, page: 655].

D. ELECTRICAL LOADS

Fig. 2 contains large electrical loads. A conventional aircraft uses bleed air for the ECS and WIPS. The ECS ensures air exchange, regulates the interior temperature, and adjusts the air pressure. In the Boeing 787, the ECS is represented by large and small compressor units and fans [32, page: 11]. The system requires a compressor capacity of $4 \cdot 100$ kW [20, page: 57].

Heating blankets replace the typical WIPS and reduce the power consumption by half. Constant anti-ice protection or sequential de-icing is achievable [32, page: 11].

The hydraulic system controls the control surfaces and landing gear. For this purpose, two large compressor units deliver a pressure of 34.5 MPa at approximately 7.95 m^3/h. Additional electric no speed controllable compressors and the main engines provide additional hydraulic system pressure. Due to the high system pressure, the hydraulic components are smaller and save space and weight [20, page: 6].

Electric components partly replace the hydraulic systems, where Electro-Mechanical Actuators (EMA) and Electro-Hydraulic Actuators (EHA) supplement the system. EHA should preferably be used for primary control surfaces, such as rudders, ailerons, and elevators. The secondary control surfaces, such as flaps and slats, are primarily responsible for efficiency and comfort. Operation via EMA is possible, although there is a risk of jamming [33, page: 3]. The brakes in the Boeing 787 can also be operated via EMA [20, page: 59].

Further optimization potential has the Electrical Taxiing, which avoids nitrogen dioxide, noise, and unnecessary fuel consumption during taxiing. Also, the aircraft is independent of ground vehicles [20, page: 61-61].

The Active Laminar Flow Control System (ALFCS) accommodates a further increase in the efficiency of a commercial aircraft. With the help of electric compressors, the aerodynamic drag of the aircraft is reduced [37].

In the next Section V, the challenges posed to a high voltage electrical power supply system by the harsh environmental influences are highlighted.

V. HVDC GRIDS FOR AIRCRAFT APPLICATION

In this section, a supply grid voltage for future AEAs will be proposed. Only DC grid structures are considered, as all energy sources in an AEA are most likely to be DC (fuel cells and batteries). Furthermore, no overrating of power converters due to reactive power is necessary and the system complexity is reduced, as most of the converters can be DC/DC converters. Inverters are only used for motor loads like flight control systems, cooling liquid pumps, e-taxi and propulsion. No rectifiers with a large volume due to power factor correction stages are needed. At first, estimations on power demand are given based on data for standard regional cruiser airplanes with a capacity of 100 pax. The overall power needed is separated in continuous and dynamic power demand. Continuous power demand is needed by lights, ECS, avionics, hotel and galley loads, and the WIPS. Dynamic loads are flight control actuation systems. The propulsion system requires a mostly continuous power during cruising, the power demand for climb and descent is higher. For the WIPS, a power demand of 35 kW can be estimated, based on data given for a Boing 787 [38]. Hotel and galley loads combine to a few kilowatts, the ECS has an estimated power demand of 150 kW [39]. For flight control systems, the peak power demand is 20 kW [40]. The demand of auxiliary power for the electrical system itself, namely pumps for liquid cooling and fuel cells, is still unknown. In total, all non-propulsive loads of a regional cruiser airplane are expected to be less than 300 kW. For a state-of-the-art MEA (Boing 787, 400 pax), the power demand of all electric loads is given as 1 MVA [20]. Compared to this number, the above estimated value seems reasonable. The largest power demand comes from the propulsion system. Here, a peak power of approximately 3.7 MW during take-off and climb, and descent can be assumed, based on conventional turbines for a short-range aircraft [41]. At cruising speed and altitude, a continuous power of approximately 0.6 times the peak power is needed [42]. Based on this data, an overall peak power demand of 4 MW is estimated. In the literature, voltage levels of 540 V($\pm$270 V) are proposed. This value is mainly determined by the currently available technology. The APU and the generators have a three-phase output with a voltage of 230 V, which can be rectified to a DC voltage of 540 V or $\pm$270 V without the need of additional DC/DC converters or transformers [10]. For future AEAs, APU and Ground Power Unit (GPU) can be replaced with newer technologies like on-board fuel cells or electric charging at the airport.

As a result, an increased voltage level of 3 kV($\pm$1.5 kV) is proposed in this paper. This has the advantage that the current per conductor is decreased, therefore, the conductor diameter is smaller. As an example, by applying a high grid voltage of 3 kV, a current of 617 A is needed to supply a peak power of 1.85 MW for one propulsor. For a lower grid voltage of 540 V, a current of nearly 3.5 kA would be necessary. Consequently, the conductor mass of high power transmission lines can be reduced by a large factor. In the same time, current stress of the semiconductors is reduced, while increasing the requirements in power electronics packaging, as a high insulation is necessary.

Especially for application in aircraft, environmental influences cause stronger restrictions than for ground applications.
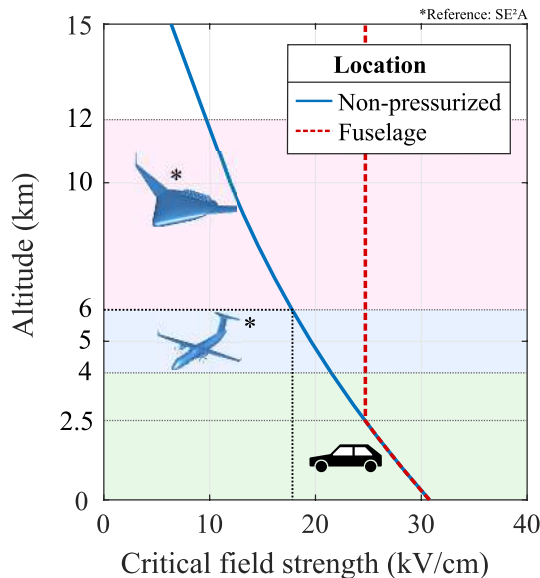
FIGURE 3. Critical field strength in dependency of altitude.

At a typical cruising altitude of 6 km for regional aircraft, the air pressure is reduced to less than half of the air pressure at sea level, while the temperature is decreased to 250 K [43]. As a result, the critical field strength is drastically reduced according to Paschen's Law [44]. This is slightly compensated by the lower air temperature, which increases the critical field strength. In the fuselage, air pressure is controlled by the ECS to a minimum value of 760 hPa, which is equivalent to an altitude of approximately 2.5 km (see Fig. 3). For non-pressurized locations, the critical field strength at a flight altitude of 6 km is reduced to $17.8 \, \text{kV cm}^{-1}$. In the fuselage, the critical field strength is $25 \, \text{kV cm}^{-1}$, as long as the ECS is fully functional. In case of failure, the pressure can even drop to ambient conditions. Power electronic systems need to be functional under these conditions. Therefore, creepage and clearance distances have to be designed to withstand the lower air pressure. This leads to special designed packages for power electronics. Another possibility is the potting of electronic systems. Consequences on the wiring harness are further discussed in Section IX.

Humidity is another environmental effect, which can have an impact on the applicability of high voltage supply grids. Energy transmission systems and power electronic devices can be affected by moisture by short-circuiting of the contacts through condensation, degrading the insulation materials for cables and silicone gel used in power electronic modules, and reducing the blocking voltage of power semiconductors through electrochemical migration and aluminum corrosion. The bias voltage has a strong impact on the lifetime of power semiconductor modules under high humidity. Devices biased at 90% of their blocking voltage capability showed an accelerated aging with a factor of two compared to devices biased at 65% of their blocking voltage capability. As power electronic devices are usually operated below 60% of their rated voltage, a long lifetime of the devices can be expected.

This is further supported by the fact that the relative humidity of the air inside the fuselage is below 20%, as it is conditioned by the ECS. For power electronic systems placed in the wings or the nacelle, dehumidifiers have to be considered as seen in inverters for wind energy systems.

Next to air pressure and humidity, radiation limits the application of high voltage systems in aircraft. Radiation effects can be caused by primary or secondary sources. Primary radiation is direct cosmic radiation (mainly protons and α-particles). At typical flight levels, cosmic radiation forms a neutron shower via spallation at atmospheric molecules, the so-called secondary radiation. As a result, damage due to radiation can be divided in two effects. Firstly, device parameters can be altered because of the Total Ionizing Dose (TID). For given travel routes, the TID can be estimated based on radiation data [45]. For example, a standard short-range flight in an altitude of 6 km can result in a radiation dose of $200 \, \mu\text{Sv h}^{-1}$ [46]. Based on published data, a strong impact of the radiation dose on semiconductors used in short-range aviation is not expected. In [47], Si Insulated Gate Bipolar Transistors (IGBT) under radiation are investigated. By using a gamma radiation source, reduced gate threshold voltage and reduced turn-on and turn-off times could be observed, combined with a higher voltage overshoot at turn-off. However, for a reduction of the gate threshold voltage of 1 V, a flight time of above three million hours under abovementioned conditions would be necessary. Current research on the effects of radiation on GaN devices is, for example, conducted by the NASA [48]. As for Si, parameter variations due to the TID are unlikely to occur during the lifetime of power devices for the application in aviation. This is confirmed by research done in [49], [50] and [51]. Under heavy irradiation, drain saturation current, transconductance and gate threshold voltage are reduced, the drain to source breakdown voltage increases. However, the proton flux used in the accelerated tests of $2 \times 10^{15} \, \text{cm}^{-2}$ is equivalent to decades of operation in low earth orbit. As a result, it can be concluded that device parameter alteration due to TID is of no significance for application in aircraft.

Secondly, power electronics can fail due to a single neutron hitting the device (Single Event Effect (SEE)). If these high energy neutrons hit a silicon ion, a conductive plasma can be formed, which spreads throughout the device [52]. This effect is dependent on the applied drain-source voltage. The device will be short-circuited by this discharge. During this time, the self-heating of the device can lead to a non-reversible destruction. As only a single event is necessary, the probability of failure depends on the availability of high energy neutrons, therefore on the neutron flux, which shows a dependency on the altitude, the geomagnetic location and on the solar activity. For a given location, the neutron flux in an altitude of 6 km can be increased by a factor of about 70, if compared to sea level [53]. As an example, estimated Failure in Time (FIT) rates for 1.7 kV SiC Metal Oxide Field-Effect Transistors (MOSFET) in dependency of the altitude are given in Fig. 4. Data is based on results in [54]. It can be
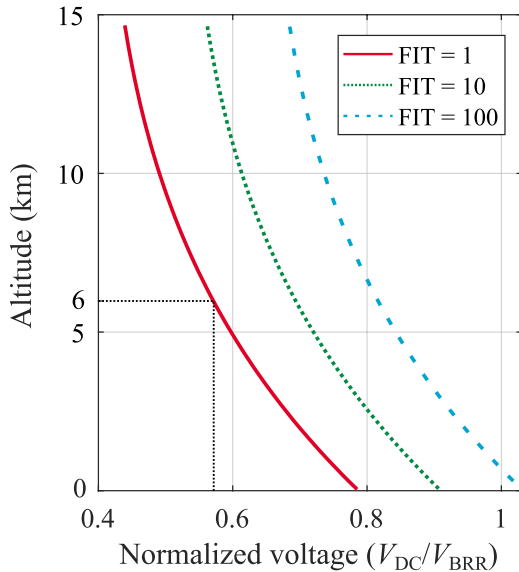
FIGURE 4. Reduction of drain source voltage for higher altitudes.

seen that in order to achieve a FIT rate of 1 (one failure in 10^9 hours) at a flight level of 6 km, the grid voltage needs to be below 60 % of the device breakdown voltage.

Generally, power semiconductors made of GaN and SiC promise better resistance to radiation than conventional silicon devices. For instance, the displacement energy of both SiC and GaN is considerably higher than for silicon [55]–[57]. More details on the behavior of GaN and SiC under radiation are given in Section VII-D. Based on the aforementioned results, for a DC grid voltage of 3 kV, semiconductor devices or combinations of single devices with a blocking voltage of at least 6 kV are necessary. For example, first versions of 6.5 kV SiC MOSFETs are currently under investigation for drivetrains in railway applications [58]. Alternatively, multilevel inverters made of devices with lower blocking voltage can be applied, for example, Active Neutral Point Clamped (ANPC), Switched Capacitor Converter (SCC), or Modular Multilevel Converter (MMC). The MMC configurations can be especially beneficial for motor inverters, as the voltage slew rate compared to conventional solutions can be reduced while still maintaining high switching speed and low switching losses [59], but they are usually of large volume and weight and therefore not suitable for aircraft applications. Nevertheless, newest research on power density improvement show significant advancements in the passive components based on quasi two level operation and nonlinear inductor designs [60]. In Section VII, more details will be given. After all, these solutions are of high complexity and investment costs, and for high voltage SiC MOSFETs, the electric performance still needs to be investigated.

Under these circumstances, a careful selection of the voltage levels is needed. As shown before, the main power demand during operation arises from the propulsion system. For this reason, a dual-zone high voltage grid is a viable solution. For supplying power to the propulsors, a voltage level of 3 kV can be selected, in order to reduce the maximum current

and therefore volume and weight of the wiring harness. For lower power loads, a DC voltage of 800 V can be sufficiently high, by still reducing wiring harness dimensions and at the same time lowering system complexity. For example, a three-level ANPC made of 1.2 kV SiC MOSFETs provides sufficient blocking voltage capability based on the aforementioned considerations on cosmic radiation. A detailed drawing of a viable grid structure is given in Fig. 5.

VI. INITIAL PROPOSAL: ELECTRICAL ARCHITECTURE FOR AN ELECTRICALLY POWERED SHORT-RANGE AIRCRAFT

This topic deals with the realization concept of an electrically powered aircraft, the necessary development steps, and the research approaches regarding electric components. An initial electrical architecture, as given in Fig. 5, is proposed. With the help of the estimations of electrification, see Section III, it can be possible to realize an electrical power of 10 MW in a high voltage electrical power supply system by 2050. Based on this initial diagram, the electrical sources, the on-board grid, and the loads are discussed.

A. MISSION PROFILE OF A SHORT-RANGE AIRCRAFT

Three different aircraft types are available: short-range, medium-range, and long-range. Mission profile data originated from the design and optimization strategy in publication [61]. The study concludes that even by optimizing the medium and short range, Flightpath 2050's targets will not be met. The short-range aircraft is far below the European Flightpath, although the overall drag of the aircraft is reduced by 47 % as a result of aerodynamic optimizations [61, page: 15]. The use of new energy storage systems and alternative propulsion concepts is proposed. In future studies, the influence of substitution by electrical components has to be investigated. With these assumptions, further algorithm-based optimization of the electrical system can be carried out. The publication [62] shows the system optimization of a hybrid-electric aircraft. In addition, fault tree analyses have to be performed in order to determine reliability. The aim is to achieve a significant weight reduction with a high fault tolerance.

Furthermore, the influence of small distributed drives on aerodynamics should be verified. It may also be possible to use free-flow drives or boundary layer ingestion. Alternative electric drives and flexible power supply create new degrees of aerodynamic design freedom [25, page: 2].

The proposal for a short-range aircraft is designed for 100 pax, has a range of 1, 000 km (540 NM) and reaches a cruising speed of 0.44 Mach at a flight altitude of 6, 000 m. Based on initial estimates, a shaft power of 3.7 MW is required and the energy storage is to be designed as a battery. Shaft power is within the technology estimation of less than 10 MW in 2050, as given in Section III.

B. ELECTRICAL SOURCES

The proposed power supply system structure includes not only batteries but also fuel cell systems. Despite the further
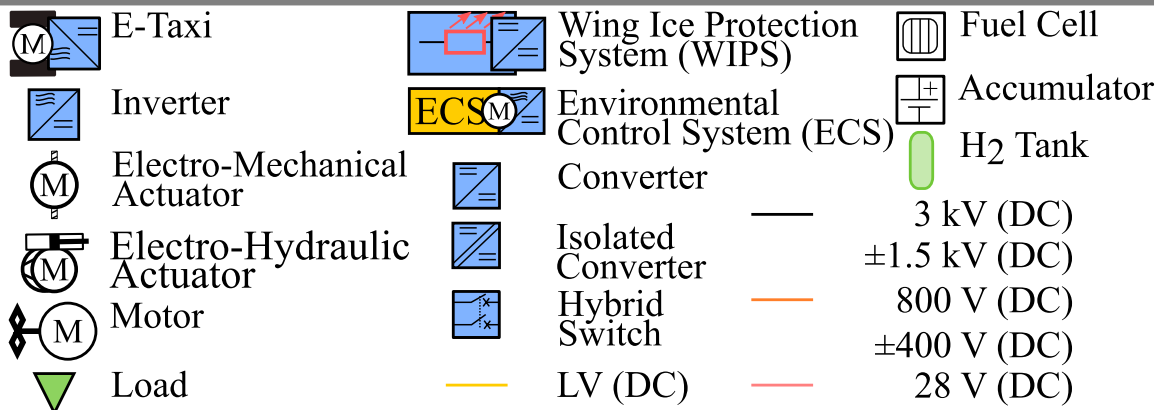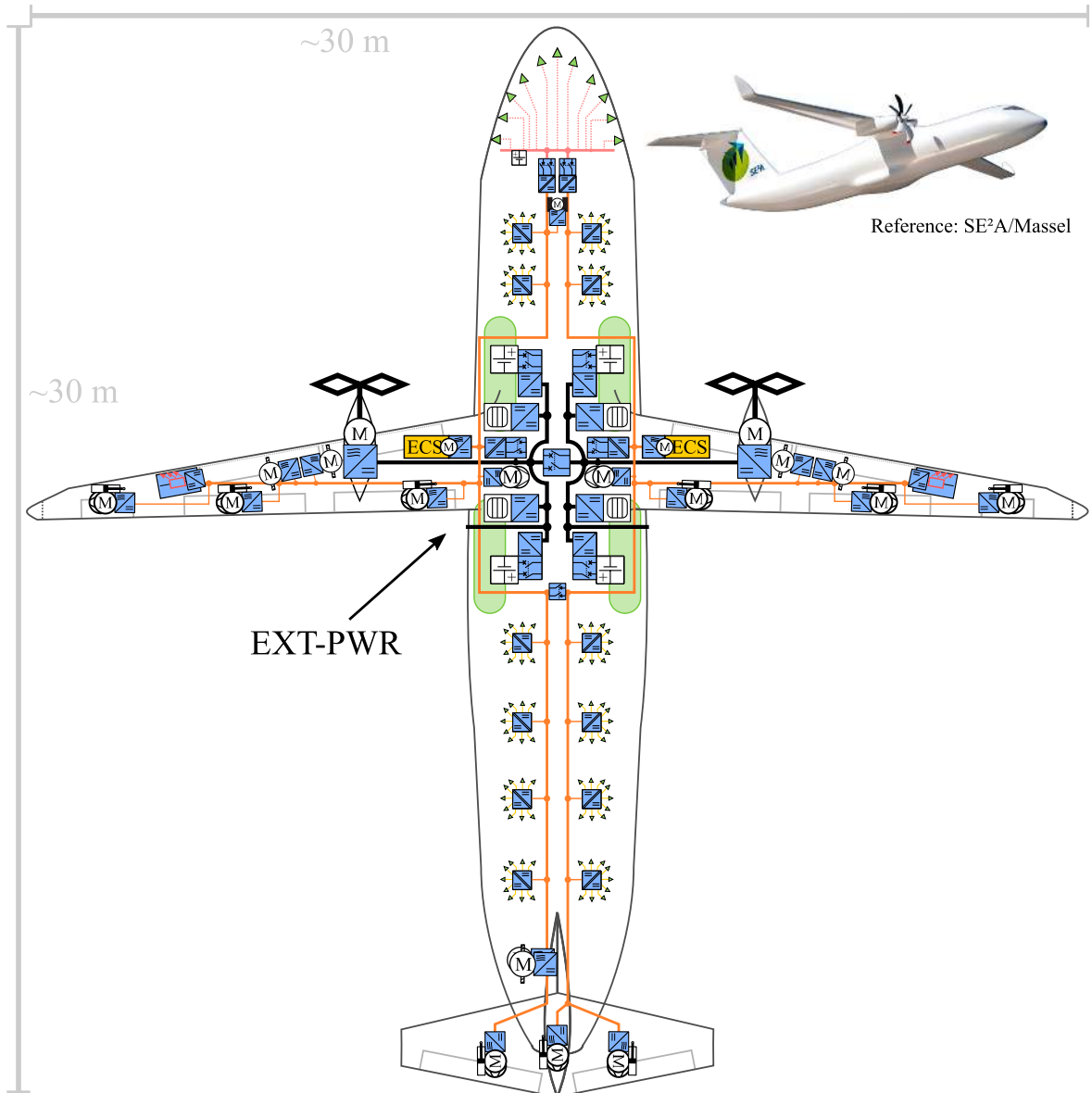
FIGURE 5. Electric schematic of AEA.

development of battery technology, the finite charging capacity at the airports is a known limitation. Little ground times require extensive charging capabilities, which must be available at the airports.

1) CHARGING AT AIRPORTS

For an estimation, a constant power of 3 MW over the entire flight profile (without take-off and landing process; without peak power) is assumed. The travel time is 1.5 h, which requires an energy of 4.5 MWh (without efficiency chain: electric machine, inverter, cable layers, converters, and battery). To get the aircraft airworthy again within 30 min (certain State of Charge (SoC)), a charging capacity of 9 MW is required. It is also assumed that five small aircrafts will be handled at the same time. This leads to an electrical connection of the airport of 45 MW only for five short-range aircrafts. 45 MW is an enormous power input for today's large European airports. Long aircraft downtimes due to a more massive fleet are not very attractive for airlines.

A replacement battery concept would be a possible alternative to avoid the aircraft downtimes. A substantial electrical output is nevertheless required, but could be well combined with regenerative energies.

The authors of this paper prefer the use of highly compressed or liquid hydrogen to overcome long downtimes. The hydrogen has to be produced from renewable energies, opposite to the conventional steam reforming process. A hydrogen economy grid could support transport from generation units (e.g., decentralized electrolyzer at wind power plants to airports). An upcoming decentralized grid needs storage facilities, whereby hydrogen production with electrolyzers could be a possible approach. Today, many wind turbines are still being phased out at low electricity demand. According to the report of the German Federal Wind Energy Association, 5.518 TWh were regulated in 2017 (wasted energy) [63, page: 2]. A significant disadvantage lies in the long and weak efficiency chains from the generation of electrical power to thrust.

2) BATTERY

The estimated technological limit for the pure use of batteries in an aircraft is a gravimetric energy density of 500 Wh/kg [64, page: 27]. Many scientists are working on increasing the energy density of batteries (2017: 350 Wh/kg [65, page: 1]). An improvement in energy density has already been achieved through the dispersing process of the sulfur cathode material and calendering process parameters for compacting the cathodes [65, pages: 6-7]. For the year 2030, a gravimetric energy density of 500 Wh/kg (volumetric energy density 1000 Wh/l) of solid-state battery (generation 4) is predicted [66, page: 9]. Another possibility is the combination of silicon and sulfur. For a fast charge, the chemical and mechanical stability for Si wires from the solid electrolyte interface is of particular interest [67]. Lithium-air batteries could also be a key technology as they promise high theoretic energy densities (year 2030+: practical densities of 500 Wh/kg $\leq$)

[64, page: 7]. With these approaches, an environmentally friendly and cost-effective battery can be built.

3) FUEL CELL

Highly compressed (e.g., 70 MPa) or liquid hydrogen is particularly interesting due to its gravimetric energy density (without tank 33.3 kWh/kg, gasoline about 11.6 kWh/kg), but is characterized by a relatively low volumetric energy density [68]. Liquid hydrogen could also be used for superconductivity in the on-board grid. Superconductivity requires very low operating temperatures, which could be ensured by the liquid aggregate state of hydrogen. The fuel cell system currently still has small power densities of 2 kW/kg [34, page: 11]. Through the use of new materials, a power density of 10 kW/kg is to be achieved for the year 2050 [35, page: 6].

A problem is its relatively poor efficiency. At the nominal point, the fuel cell has an efficiency of about 60 %. For example, assuming the fuel cell stack has an electrical output power of 3 MW, there is a waste heat output of 2 MW. A portion of the resulting waste heat can be used as heat output for the WIPS and ECS. Dissipating unused heat from the aircraft will be a challenge for the entire aircraft design. Waste water can be partly used as service water. However, the unused water in the aircraft cannot be drained during the flight phase; it has to be stored.

For the application of fuel cells in aviation, the functional reliability and the hazard-free operation has to be ensured. It can be deducted, that fuel cells are generally suitable for the application in any vehicle propulsion. Fail-safe operation can be guaranteed by paralleling multiple fuel cell systems as shown in Fig. 5. Hydrogen used as fuel has to be considered as potential safety hazard. Hydrogen will leak faster through breaches in the storage tank than any other gas. As a result, tanks have to be closely monitored during operation and maintained regularly. Small quantities of escaped hydrogen are relatively harmless because it disperses rapidly and is therefore unlikely to accumulate in the concentration required for detonation. The ignition temperature of 560 °C is higher than for jet fuel, but, like other gases, hydrogen can always be ignited by a spark. In the end, hydrogen poses similar safety hazards as other liquid and gaseous fuels and needs therefore to be handled with special care.

4) COMBINATION OF FUEL CELL AND BATTERY

The wiring system topology in Fig. 5 contains four fuel cell systems with batteries to overcome long downtimes. The wider fuselage contains the batteries and fuel. Two source combinations are responsible for one side. From the mission profile-based analysis, the constant performance during the flight phase is to be covered by the fuel cell system. With the help of the batteries, the peak load during take-off is covered. The fuel cell is kept at a power level as constant as possible so that the battery can also be charged by the fuel cell system during flight operation. When landing, the battery is charged more strongly due to the low required load. This approach

only needs a low charging power to be applied during ground time. Further operating strategies are conceivable.

Circuit breakers are represented by the hybrid switch, which provides galvanic isolation. Disconnecting DC circuits is a challenge because of the lack of the natural current zero crossing. The hybrid circuit breaker is mounted directly on the batteries in order to be able to switch off quickly and without large cable impedance in the event of a short circuit. The short-circuit behavior of the fuel cell is currently being investigated.

In order to integrate the fuel cell in an optimal operating window and into the high voltage electrical power supply system, a power electronic converter (MEA, 2013: 5 kW/kg [69, page: 10]) is required. The stack level of the cells has a significant influence on the converter topology.

The integration of the batteries into the electrical power supply system is also significantly influenced by the stack level. The question arises whether a converter is necessary here. Without converters, the high voltage electrical system voltage would be dependent on the SoC of the batteries. In addition, load flows and SoC of the distributed battery systems can be better controlled by power electronics. A large number of variants to integrate fuel cells into the on-board power supply system is possible. Further investigations have to be done.

C. ELECTRICAL DISTRIBUTION SYSTEM

The electrical power supply system, as given in Fig. 5, consists of two primary voltage levels (3 kV and 800 V). DC voltages are preferred to decouple sources and loads. We propose several voltage levels. Power electronic converters enable an energy change between several voltage levels.

1) 3 kV DC VOLTAGE

The 3 kV level (± 1.5 kV) connects the large loads, especially the electrical drive of the aircraft. The sources should be located very close to the inverters, which enables the shortest possible cable lengths.

The voltage for the transmission of such high power should be as high as possible to reduce weight. The design of the insulation is an essential criterion for avoiding arcing. Due to the harsh environmental conditions (temperature, humidity, and pressure), creepage and clearance distances change drastically, as given in Section V. It represents a significant challenge for the design of power-dense power electronics and electrical machines.

Evidence of safe operation must be provided in further investigations - the voltage level results from the possible breakdown voltage capability of future wide bandgap semiconductors (6.5 kV). An important design criterion of power electronics is the consideration of cosmic radiation, as given in Section V. As there is a less danger due to cosmic radiation during ground time (sea level), it would be possible to increase the on-board voltage for a possible charging process (e.g., 3.6 kV or even higher).

2) 800 V DC VOLTAGE

A hybrid circuit breaker allows disconnecting the power supply in the event of a fault. Two isolated converters generate the 800 V (± 400 V) level, which is available for smaller loads. The insulation is less complex compared to 3 kV (± 1.5 kV). The approach is to be close to the voltage in automotive, photovoltaics, etc. SiC semiconductors with a breakdown voltage of 1700 V are preferable, as given in Section V. Otherwise, a combination of SiC and GaN can be used to achieve a higher power density. A high power density could also be reached in this power range (100 kW $\leq P <$ 200 kW) by a pure GaN approach.

The mains can be separated by two hybrid circuit breakers in case of possible fault conditions. Another hybrid circuit breaker can separate the grid structure in the event of a major failure.

3) LOW VOLTAGE LEVEL

The 28 V on-board power supply for the avionics is generated from the 800 V (± 400 V) on-board power supply. Two isolated converters are available to generate the 28 V. A hybrid circuit breaker per string ensures fail-safe operation.

Distributed isolated converters provide electrical power for the galley, multimedia applications, lighting, etc. The converters connect the 800 V electrical power supply with the low DC voltage.

Converters based on GaN are beneficial for generating the low voltage level and the 28 V for avionics. High switching frequencies (200 kHz $\leq f_s <$ 1 MHz) at lower power levels can lead to very power-dense converters.

D. ELECTRICAL LOADS

The largest electrical load is represented by the electrical drives (electrical machines 2017: 10 kVA/kg, 2050: 40 kVA/kg for long-range aircraft [23, page: 655]) generating the thrust. An output of 3.7 MW of mechanical shaft power per engine is required. The publication [70] presents a hybrid ANPC inverter (SiC and Si) with a power density of 12 kVA/kg. A summary of NASA's research projects on new machine concepts and inverters with very high power density data is given in the publication [71]. For example:

- Inverter: General Electric
    - continuous power: $P_N = 1$ MW
    - specific power goal: 19 kW/kg
- Electrical Machine: NASA Glenn Research Center
    - continuous power: $P_N = 1.4$ MW
    - specific power goal: 16 kW/kg

The smaller loads are the ECS ($P = 150$ kW) and the WIPS ($P = 35$ kW), as estimated in Section V. The primary and secondary control surfaces are operated by EMA, EHA. Hydraulic pumps, which generate the system pressure, are also used. The hydraulic system supplements the operation of the control surfaces and enables the landing gear to be extended.

For emission-free taxiing, an inverter-controlled wheel hub machine is available. Furthermore, distributed isolated converters generate a DC voltage for small low voltage loads.

VII. POWER ELECTRONICS

The AEA proposal, as given in Fig. 5, contains many power electronic components, such as different DC/DC converters and inverters.

This publication focuses on DC/DC converters in the on-board power supply system of an AEA. Different types of converters are required for the DC on-board power supply to operate at different voltage levels.

Hybrid circuit breakers are another field of application for power semiconductors. The DC on-board network requires circuit breakers which can safely disconnect parts of the power supply in the event of a fault. Hybrid switches use Silicon (Si)-based semiconductors to extinguish the arc, as given in Section VIII.

In aviation, semiconductors are subject to harsh environmental influences, such as low temperature, low pressure, low humidity, and cosmic radiation. The replacement of conventional components requires a particular high power density. Besides, the components have to be fault-tolerant and highly reliable. Special conditions and component targets are contrary.

A. SEMICONDUCTOR TECHNOLOGY

Applications differ in power and voltage range. The most suitable semiconductor is used, which allows the highest efficiency in this power and voltage range at a specific switching frequency. Fig. 6 shows the different power levels correlating with their typical range of switching frequencies and the typically used semiconductor. The physical limit of silicon-based components in terms of high power and high switching frequency is reached. The power density of components is a particular focus of aviation. A high switching frequency of the semiconductors enables a weight reduction of passive components. Further essential criteria are the current carrying capacity and the voltage blocking capability of the semiconductors. Materials, such as SiC and GaN, offer an increase in the working range due to their physical properties. Silicon-based semiconductors also continue to be of interest for some components.

1) SILICON

Silicon-based semiconductor components have been under continuous development for almost 50 years. This technology has opened up a multitude of different fields of application. The further development of various technologies, such as IGBT and Si-based MOSFET, covers a wide power range.

For example, Si MOSFETs with trench gate structures dominate the market up to 600 V [72, page: 1]. A further optimization of the MOSFET structure is the so-called super junction.

The IGBT covers a market segment from 600 V to 6.5 kV. For blocking voltages up to 6.5 kV, the IGBTs are based on a
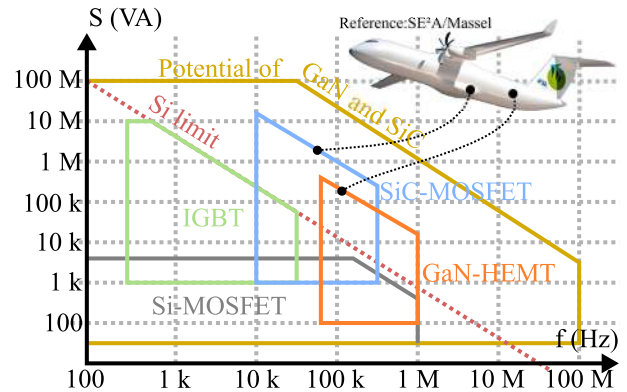

FIGURE 6. Wide bandgap semiconductor vs. Si-based semiconductors.

field stop and injection enhancement. However, the IGBT has reached its physical limits of the blocking voltage capability at 6.5 kV. The silicon-based components have an operating temperature of less than 175 °C, and the switching speed is limited [72, page: 1].

The reliability of the components has been dramatically improved through the manufacturing process and the mounting and joining technology. Furthermore, the parts have been tested over many years in a wide range of applications [72, page: 1].

2) SILICON CARBIDE

SiC, a wide bandgap semiconducting material, could be a possible technology to achieve high power densities. The hexagonal crystal structure 4H offers the largest bandgap of SiC compounds. Compared to Si, there is not only a higher bandgap, but also a better thermal conductivity due to the smaller intrinsic carrier density. Furthermore, there is also a higher critical field strength of SiC, which leads to a smaller drift layer thickness. A smaller chip area with equal conduction resistance can be achieved by high doping of the drift layer. The smaller chip area, in turn, leads to lower parasitic capacitances, enabling a higher slew rate [72].

In addition to the abovementioned excellent properties of SiC, the compound has a stable native oxide. However, in the early beginning of the SiC technique, only low channel mobilities could be achieved. The problems were high interface trap densities. A significant reduction of the trap densities at the SiC/SiO_2 interface was achieved by post-oxidation annealing in the manufacturing process in NO gas. Trap densities could be further reduced by a combination of NO and hydrogen annealing [73].

In many applications, such as regenerative energy technology and electric mobility, market entry has been expected for years. SiC wafers are 30 times more expensive than Si wafers (data of the year 2015). The production is very complicated because SiC has a polytypism crystal structure and extreme thermodynamic properties [72], [74]. CREE has planned a factory for 8" wafers in 2024 (currently 6") [75]. Si is available in 12" wafers.

There are many different optimization approaches, which can be applied to achieve weight reduction using SiC. The smaller losses (switching and conduction losses) and the higher operating temperature can lead to a reduced cooling effort. Otherwise, a higher switching frequency can be used with the same power dissipation compared to Si counterparts. The increased switching frequency leads to a drastic reduction of the passive components. On the other hand, for high-switching speed applications, Electromagnetic Compatibility (EMC) must be taken into account [72].

For the substitution of conventional propulsion systems, high power densities must be achieved. SiC could represent a solution in high blocking voltage ranges to realize a highly power-dense electrical power train.

The proposed on-board electrical system structure in Fig. 5 contains converters with very high electrical power. Especially the converters for connecting the fuel cell and the battery to the high voltage electrical power supply system (3 kV) have to deliver very high power. Two high power electronic converters generate the second system voltage level 800 V.

Today, SiC modules or discrete components are commercially available up to 1.7 kV. The cosmic radiation requires a reduction of the level of the blocking voltage [72, page: 2]. For a 3 kV DC electrical power supply system, at least four commercially available series-connected switches are necessary.

In different investigations, different manufacturers have investigated modules or discrete components up to 15 kV. Those semiconductors are not commercially available by now. The architecture of these semiconductors is planar. The blocking voltage of 6.5 kV is particularly interesting for the use in the proposed aircraft electrical system, as given in Section V. In the publication [76], ROHM Semiconductor presents a metrological comparison using double-pulse testing of 6.5 kV Si IGBTs and SiC MOSFETs. In comparison to the Si IGBT counterpart, a 75 % loss reduction is achieved. Mitsubishi's publication [58] offers the full SiC power module (so-called HV100, half-bridge module) with integrated Shottky Barrier Diode (SBD) in SiC MOSFETs. One of the emphasized features of the module is its power density. Also, the integrated SBD leads to minimal turn-off losses. The 6.5 kV SiC semiconductor presented by CREE reduces switching losses by a factor of 10 under the same thermal environmental conditions as a commercial IGBT [77]. Additionally, the publication offers a comparison of different gate runner designs. The semiconductor manufacturer CREE supplies the first verifications (ramped time-dependent dielectric breakdown) for the reliability of the gate oxide. Besides, 10 kV and 15 kV SiC MOSFETs are also demonstrated [78]. A power electronic transformerless design with 15 kV SiC MOSFETs is shown for a medium voltage application. Due to the use of high-blocking switches, there are high slew rates ($170 \, \mathrm{kV \mu s^{-1}}$) [79]. The publication [79, page: 5] highlights the parasitic ground currents over 10 A caused by those high slew rates and unwanted ground capacitance.

TABLE 1. Comparison of high voltage blocking SiC devices.

Manufacture	Mitsubishi	Rohm	CREE
Technology	Module	Chip	Chip
V_{BRR} (kV)	6.5	6.5	6.5
$T_{\mathrm{j,test}}$ (°C)	175	125	25
$R_{\mathrm{G,ext,on}}$ (Ω)	1.0	100	1.6
$R_{\mathrm{G,ext,off}}$ (Ω)	0.5	100	1.6
V_{DD} (kV)	3.6	3.6	3.6
I_{D} (A)	400	32	30
E_{on} (mJ)	410	105	12.2
E_{off} (mJ)	110	38	1.79
E_{rec} (mJ)	10	-	-
t_{on} (ns)	59	962	49
t_{off} (ns)	-	509	46

A comparison of the high blocking semiconductors is shown in Table 1. The turn-on and turn-off energy losses result from double-pulse tests of the manufacturers [58], [76], [77]. It is difficult to compare the data because the semiconductors were measured under different environmental conditions and in different test setups (e.g., $T_{\mathrm{j,test}}$). Another difference is the package technology (e.g., single test chip or module). Several parallel-connected single chips can form a switch in a module (e.g., single switch half-bridge, full-bridge). In module configuration, higher gate resistances are used to enable the parallel-connected single chips to be switched on simultaneously. Furthermore, the packaging and joining technology is more complicated, which leads to parasitic components (e.g., parasitic inductances in the commutation mesh).

An estimation of the maximum permitted switching frequency depends strongly on the packaging technology and the design of the cooling system. In the publication [77, page: 249], switching frequencies above 10 kHz are mentioned for hard switching applications. With soft-switching converters, a further increase of the switching frequency is possible.

A further step in the development of high blocking SiC semiconductors is the transition from planar structures to the so-called trench gate. It allows the chip area to be further reduced. The chip size, in turn, influences parasitic capacitances, which affect the switching behavior. In the trench gate, the gate oxide must be shielded from the high electric field strengths. The MeV Al+ implementation enables the insertion of hexagonal buried p-base regions [80].

With newer methods of packaging and joining technology based on sintering, smaller leakage inductances, higher reliability concerning mechanical stability in temperature swings, and a higher power density of the power modules can be achieved. Concerning the high voltage slew rates, a further reduction of the parasitic leakage inductance is necessary [81].

3) GALLIUM NITRIDE
Power semiconductors made of GaN are commercially available for low voltage ($V_{\mathrm{BRR}} < 200 \, \mathrm{V}$) and grid applications ($V_{\mathrm{BRR}} = 650 \, \mathrm{V}$). They have found first commercial application for low power DC voltage supplies for server or telecom

equipment. An application in an aircraft design is not known to this date. Benefits of using GaN power switches are due to their low output capacitance caused by small device dimensions [82]. As a result, they are especially suitable for high frequency operation. Size and volume of passive components can be reduced, which is a key advantage for the application in aircraft [83]. This weight and volume reduction has a huge impact on the whole aircraft system. Savings can also be due to higher efficiency and therefore lower cooling demand [84].

Manufacturing is currently done on Si substrates due to availability, low cost and the possible use of known CMOS processes. For 650 V devices, wafer sizes up to 8" are used with a yield of up to 97% [85, page: 4]. Current research trends include the integration of functional blocks (gate driver, sensors, passive components) with power devices in one chip [86] as well as higher blocking voltage devices. In this respect, poly-AlN is investigated as buffer material, as its thermal coefficient of expansion is closer to that of GaN. As a result, higher quality GaN buffer layers with a thickness of 725 μm can be grown, enabling a higher breakdown voltage [85, page: 5].

B. RELIABILITY AND SAFETY

For use in aircraft with enormous electrical powers, more investigations and optimizations have to be done. A particular focus is on the reliability of the components. The design of power electronic switches, passive components, solder joints, and microelectronics in a power electronic converter must be reliable over their entire service life. The service time of an aircraft under harsh environmental conditions is 100,000 hours [87, page: 2].

The problems of cosmic radiation, humidity and minimized pressure have already been discussed in the previous Section V.

In the Focus Point Matrix in the publication [87, page: 5]., the stressors vibration and mechanical shock on power electronic components are rated as secondary. Average temperature, temperature cycle, and humidity are more essential stressors. Further experience to prevent mechanical stress has been gained in the automotive industry. Passive components or bus bars are often mechanically stabilized with gap filler. An additional degree of freedom is also offered by the location of the components in the aircraft design to prevent mechanical stress. Test cases are listed in MIL-810.

SiC semiconductors currently have unreliable gate oxide, which has not yet been completely solved. The issue of gate oxide reliability in SiC components is well known. The relatively high error rates are due to the high field strength at the gate oxide. In literature, there are many investigations on this topic, whereby some investigations contradict or complement each other. The failures are divided into intrinsic and extrinsic models. For the intrinsic model, there is a built-in gate oxide weakness in the metal-oxide-semiconductor structure, which could be caused by trap-assisted tunneling. These studies refer to time-dependent breakdown data. Thus, the oxide on SiC can never have the same reliability as the oxide on Si.

The extrinsic model states that growing lower defect substrates increases reliability. It requires cleaner oxide or defects during fabrication have to be reduced [88, pages: 3-5]. [88] and [89] argue against intrinsic defects. The publication [89] determines the oxide reliability using the Weibull distribution for extrinsic defects. The publication [90] points out that extrinsic errors are also still caused by local high electric field strengths. In another publication [91], three error mechanisms are identified using the Weibull distribution on 3C-SiC MOS capacitors. Two error mechanisms are of extrinsic nature (fabrication). The third mechanism occurs in this study at high field strengths (>8.5 MV/cm) and is due to electron impact ionization in SiO_2.

The semiconductor manufacturers have different states in the gate oxide reliability. SiC is a young technology (approx. 16 years) compared to Si (approx. 70 years), and further field experience will be gained. Oxide reliability remains a problem.

The stability of the threshold voltage of SiC MOSFETs is essential. There are two phenomena to be separated, threshold hysteresis and bias temperature instability (bti). Hysteresis is an intrinsic and reversible effect. With the help of a reduced negative gate-source voltage, the hysteresis loop can be kept very small. Through a procedure presented in the publication [92], long-term drift effects by bti can be separated from hysteresis effects. The drift of the threshold voltage caused by bti is known and can be predicted. It is possible to consider loss changes of SiC power semiconductors and increased junction temperature stress over product lifetime.

The reliability of GaN devices is under current investigation. Results in [94] and [95] promise a high reliability of GaN devices under hard environmental conditions. Commercially available 650 V devices are qualified according to the JEDEC Solid State Technology Association (JEDEC) tests including 1000 hours of high temperature reverse bias [96].

C. SHORT-CIRCUIT CAPABILITY

The short-circuit current capability of the SiC components is also an essential criterion for the power electronic component. Si IGBTs offer a higher short-circuit current capability compared to SiC MOSFETs. The chip areas of SiC MOSFETs are smaller, resulting in a smaller Short-Circuit Withstand Time (SCWT), and Critical Short-Circuit Energy (CSCE). Very high junction temperatures (over 1500 °C) may be present, depending on the investigation [93]. Trench gate structures have a small short-circuit current capability due to the smaller chip area and the associated higher current densities [97]. It is possible to use intelligent and fast driver concepts to prevent the destruction of the semiconductor.

The behavior of GaN devices under short-circuit conditions is under current investigation. A strong dependency of the carrier mobility on the device temperature is characteristic. As a consequence, the drain current is strongly decreased after reaching the initial saturation current, due to high initial losses and therefore a strong self-heating of the device, which will reduce the drain saturation current.

Additionally, the strong heating of the device leads to a large gate leakage current, which will decrease the gate voltage and by that further reduce the drain saturation current. These two effects act as negative feedback and help to increase the time to failure during short-circuit occurrence [98]–[100].

Next to the device temperature, the behavior of GaN switches during short circuit is strongly dependant on the applied drain to source voltage. In [99], enhancement mode GaN switches with a rated voltage of $V_{DS} = 650$ V were tested. These switches will typically be applied at a DC link voltage of 400 V. It could be demonstrated that for reduced DC bias below 350 V, the devices could withstand more than 10 μs under short circuit. After increasing the DC bias to 400 V, the time to failure was reduced to 600 ns, which is far less than delay times of typical short-circuit protection measures. By decreasing the gate voltage to $V_{GS} = 4$ V compared to the standard 6 V, the time to failure could be extended above 10 μs, again due to the negative feedback effect explained above. However, as this will also increase conduction losses during normal operation, it is not a feasible measure to increase the robustness to short circuits.

The actual physical mechanics during short circuit are currently investigated as well. For depletion mode GaN devices, the device temperature at failure did not exceed 150 °C, as presented in [100]. As a result, a thermal failure of the device was rejected as primary cause for the device destruction. Instead a accumulation of holes due to impact ionization during short circuit could lead to a destruction of the gate structure. For the preferred enhancement mode devices, deeper analyses of the failure mechanism are still to be done. But generally speaking, the currently available lateral GaN switches show much smaller time to failure than comparable Si and SiC switches. Therefore, the improvement of the device structure of GaN switches to enhance the short-circuit robustness is an important task for future developments.

D. COSMIC RADIATION

For SiC devices, the trench gate structure and the associated chip size reduction have a positive contribution to robustness against cosmic radiation. With a smaller chip area, the probability of contact of the chip area with a neutron is reduced. A substantially reduced operating voltage to the blocking voltage prevents damage due to cosmic radiation. The semiconductors must also be well cooled in order to reduce the dielectric strength of the chip. Thus, the latching sensitivity can be minimized. Furthermore, the choice of topology as well as the design strongly affect the robustness against cosmic radiation. A long duty cycle of the semiconductors minimizes the probability of cosmic radiation-based destruction during the blocking phase. The semiconductor should be conductive for as long as possible over the switching period. It reduces the probability of a parasitic turn-on by a neutron [101], [102].

Especially radiation hardness is in favor of GaN devices over conventional silicon semiconductor. Parameter alteration due to irradiation (TID) can be observed for gate threshold voltage, drain saturation current and drain source breakdown voltage [51]. However, the here applied doses far exceed any possible radiation dose during flight operation. Consequently, TID is of no significance for aircraft operation. For SEE, first results have been gained by simulation in [49]. One effect is that, after impact of a neutron, a conductive plasma is formed in the active region of the device. Hereby, a parasitic bipolar transistor can be turned on (Single Event Burnout (SEB)). This effect seems to be of minor significance for GaN devices. Secondly, charge accumulation below the gate is possible. Both mechanisms only lead to a transient triggering of the device, the drain current cannot be sustained, thus, a device burnout is avoided. The highest effect on the drain current amplitude is by the drain source voltage bias during the neutron impact. Other factors, like the location and angle of impact as well as the penetration depth, show lower impact. For a voltage bias close to the rated voltage, a large displacement current occurs after the heavy ion impact. This current can reach values of 0.1 A μm^{-1} and leads to the thermal destruction of the device. Also, Single Event Gate Rupture (SEGR) has been found to be a possible reason for a SEE in GaN devices. After all, GaN High Electron Mobility Transistors (HEMTs) are generally more radiation robust than silicon counterparts, as stated before [55]. As a result, radiation hardening of the devices can possibly be avoided. This process usually decreases the electrical performance of the device massively. If the radiation hardness of GaN can be confirmed in further studies, their application in aircraft systems has to be preferred over silicon and maybe also silicon carbide devices.

E. TOPOLOGIES

There are many restrictions on the design of a DC/DC converter in aviation; some of them are contradictory. In particular, the harsh environmental influences, such as air pressure, temperature, and humidity, affect the clearance and creepage distances within the converter have to be considered. More considerable distances between individual conductors inevitably lead to larger leakage inductances, which must be kept as low as possible for switching losses and immunity to cosmic radiation. Parasitic inductances and high rates of current change can lead to voltage overshoot at semiconductors. By the use of wide bandgap devices, a reduction of the heat sink effort can be achieved. Additionally, the cosmic radiation must be considered, as it significantly influences the power density of the converter.

Section VII-A2 deals with the issue of high slew rates and the resulting Electromagnetic Interference (EMI). A trade-off has to be found between switching speed (losses in the semiconductor and cooling effort / minimizing passive components) and the EMC (filter efforts and shielding) of the DC/DC converters.

A converter design might have parasitic ground capacitances, which can lead to problems in EMC. For example, a semiconductor module can have a large parasitic capacitance of the switching node/capacitive node against the
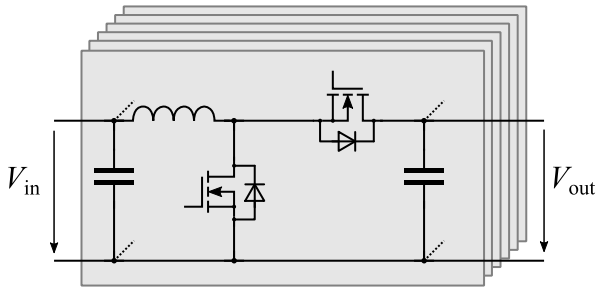
FIGURE 7. Interleaved step-up converter.

backside of the Direct Copper Bonding (DCB) or a large parasitic capacitance against its base plate.

Furthermore, all components must be designed to be as fault-tolerant (sum of all catastrophic failures of aircraft: FIT: $1 \cdot 10^{-7}$) and reliable as possible [34, pages: 6-8]. The design of the converter from passive and active components is very challenging under the influence of the requirements and conditions mentioned above.

1) NON-ISOLATED CONVERTERS
A non-isolated topology could be used to integrate the sources into the electrical power supply system. In publications [69] and [103] on a MEA and a fuel cell-powered small electric aircraft, step-up converters are used. The converter for the battery has to be bidirectional to enable charging and discharging, while the converter connecting the fuel cell can be unidirectional [69], [103].

Fig. 7 shows a step-up converter that can be further optimized by interleaving, synchronous rectification, and coupled inductors. For maximum efficiency of this converter, the input voltage should be as close as possible to the output voltage. This requirement affects the stack level of the battery and the fuel cell. The converter is characterized above all by a small number of semiconductors; half-bridge modules can be used. Additionally, good scalability and modularity can be achieved utilizing interleaving. Also, it is easier to integrate smaller inductors into an existing cooling concept. Due to the multiphase principle and the use of specific duty cycles, ripple currents of the sources are minimized by cancelling effects. With the aid of the coupled inductors, a further size reduction of these is possible [104]. A very powerful interleaved step-up converter (100 kW, input voltage 600 V, without EMI filter) for automotive applications is presented in [105]. A power density of 25 kW/kg is achieved with commercially available devices. The publication [69, page: 10] presents a DC/DC converter for a MEA with a power density of 5 kW/kg.

As both rated current and rated voltage are typically lower for GaN devices compared to available SiC MOSFET and Si IGBT, the application will be limited to low and medium power converters, if not massively parallelized. The usage of smaller distributed converter systems requires a suitable grid structure, but will also lead to a more meshed and redundant supply grid [106]. As shown in Fig. 5, small Point of Load
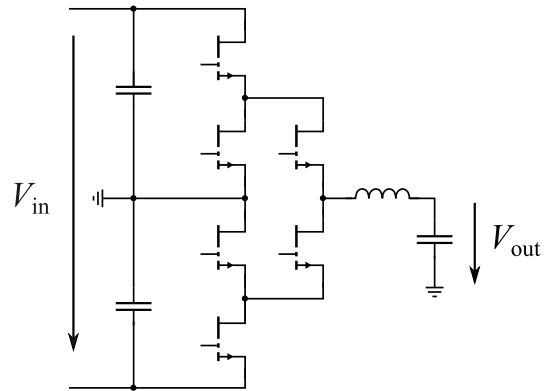

FIGURE 8. GaN-based ANPC inverter for an input voltage of 800 V (±400 V).

(PoL) inverters can be used for supplying avionics, hotel and galley loads from a 800 V DC grid. To take into account the reduced maximum breakdown voltage due to cosmic radiation, multilevel inverters with five levels need to be realized based on the currently available devices, even for a 800 V DC grid. As devices with higher voltage rating will be available in the future [85, page:5], device count can probably be reduced. SCC are especially promising. Because of the reduced inductance value and lower device stress, they can be designed towards high power density at a high voltage gain and relatively high efficiency, but come with high requirements in their design and especially EMI aspects [107]. For higher power demands, ANPC converters can be used with paralleled output stages (see Fig. 8). While GaN devices principally allow parallelisation [108], filter design and layout considerations can be simplified by using interleaved GaN half bridges. By using a high number of interleaving stages, the system redundancy is increased as well. As a drawback, a high number of inductors is necessary, but typically with less overall weight and volume due to a partial compensation of the ripple currents. For higher blocking voltages, MMC can be used. Conventional MMC require large module capacitances and are therefore not suited for weight- and volume-sensitive applications. By using the so-called quasi-two-level mode, module capacitance can be drastically reduced [109]. After detailed study, these systems could find an application in future AEA supply grids.

2) ISOLATED CONVERTERS
Fig. 9 shows a possible topology of an isolated DC/DC converter. The Dual Active Bridge (DAB) is a bidirectional isolated converter and conventionally consists of four half bridges. Due to high switching frequencies, the weight and volume of the transformer can be reduced. The transformer can achieve a significant voltage amplification ratio, with respect to the possible stack level. In comparison to the non-isolated converter, there is an increased complexity.

The leakage inductance is mainly responsible for the transmittable power. The soft-switching operation of DAB can be achieved with the resonance of leakage inductance and
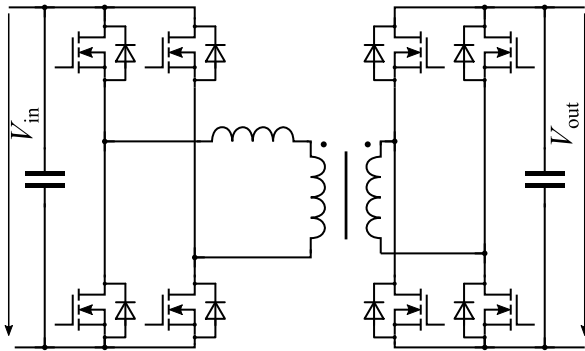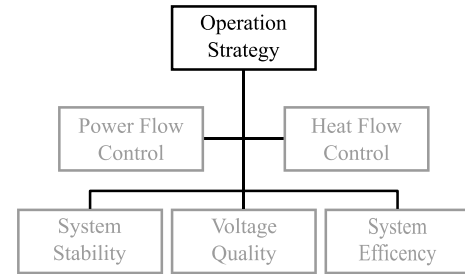
FIGURE 9. Dual active bridge.

FIGURE 10. Operation strategy for a reliable AEA system.

FIGURE 11. Possible services provided by the protective devices in various failure scenarios.

drain-source capacitances. The semiconductors on the inverter side (depends on power flow) can operate under Zero Voltage Switching (ZVS). It allows switching losses to be reduced, less cooling is required, or higher switching frequencies are possible. ZVS is determined by the charging process of the drain-source capacitances and the leakage inductance. ZVS cannot be achieved for the entire working range under the standard Single Phase Shift Modulation (SPS). The limitation lies in the magnetically stored energy in the leakage inductance. The semiconductors are in a blocking state over half of the duty cycle [110]. Power transmission using phase-shift modulation has advantages concerning cosmic radiation. The duty cycle of the semiconductor in this modulation method is a maximum of 50 %. An optimized control strategy of DAB is the Expand Phase Shift Modulation (EPS), which increases the operating range of the ZVS and minimizes circulating currents. Triple Phase Shift Modulation (TPS) has three degrees of control, extends the ZVS range to no load, reduces RMS currents and peak currents, and minimizes the transformer. Another option is a multiphase system [111].

The publication [112] presents a 100 kW isolated DC/DC converter for renewable energies with a power density of 1.2 kW/kg (air-cooled, not gravimetric or volumetric power-dense optimized).

The switching frequency of the DAB can be further increased with a resonant tank consisting of a capacitance and an inductance on each side. It is also known as the CLLC converter. The variable switching frequency between two resonant poles allows the output voltage to be adjusted. Zero current switching is available on the rectifying side. A disadvantage in contrast to DAB is the low bidirectional transmission speed [111]. One challenge of the CLLC converter is synchronous rectification [113]. For an accurate standard Fundamental Harmonic Analysis (FHA), the highly voltage-dependent output capacitances of semiconductors have to be taken into account. The output capacitance of many semiconductors changes during the switching process. Furthermore, no loss calculation is possible with the standard FHA methodology, but a loss calculation is essential for a power-dense design of the converter. Publication [114] enables a loss evaluation in the time domain. The time domain enables a loss consideration to be carried out in the same way as for
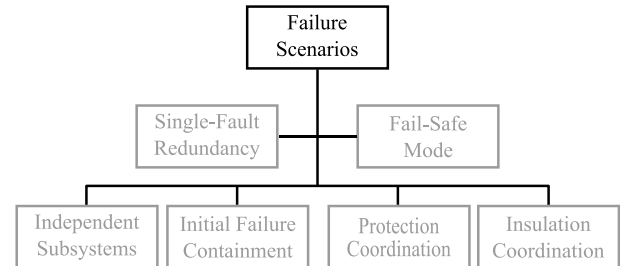
designs of other converter types. In addition, it is challenging to handle various input and output voltages.

VIII. TECHNOLOGIES FOR CIRCUIT BREAKERS FOR AEA
Within the aircraft proposal, Fig. 5, switching operations have to be performed to connect and disconnect parts of the electrical power supply system in the event of occurring failures. In this section, the safety component Circuit Breaker (CB), its need and function will be discussed. Subsequently, different concepts will be compared to determine an optimal solution for the technical requirements in AEA. Then different technologies for this solution will be discussed and assessed regarding the special requirements. Furthermore, the environmental influences on the components will be outlined.

A. HIGH VOLTAGE SWITCH REQUIREMENTS IN AN AEA
To reduce the losses in the wiring harness and the weight of the distribution equipment, higher voltages above the low voltage level are needed, Section V. This leads to different equipment in the aircraft which is basically known from the high voltage technique.

The operation strategy and possible failure scenarios of the European Plan for Aviation Safety EPAS define the requirements concerning future circuit breakers.

On the one hand, the operation strategy of the EPAS has to control and ensure multiple values and system parameters, as can be seen in Fig. 10.

Hence, future circuit breakers must provide a low on-state resistance to increase the efficiency. Furthermore, for the inclusion into the operation strategy, they have to be remotely switchable by a control unit or the staff.

On the other hand, all possible failure scenarios have to be recognized, they lead to additional requirements concerning future switches. Thus, multiple factors have to be considered within a failure assessment, Fig. 11:

Generally, circuit breakers within an aircraft have different tasks to fulfill, the first priority of the operation strategy is to ensure a reliable energy distribution during the whole operating time by controlling the power flow. The most challenging operation is a switching operation during an occurring short-circuit failure which has to be fullfilled by the circuit breaker. For nominal switching operations, an integration into an intelligent control unit is recommended to enhance its functionality. Furthermore, a fail-safe mode of the circuit breaker is needed to exclude the operation of a damaged breaker by ensuring a full galvanic separation.

However, circuit breakers are available for DC currents at this voltage level but they do not meet the requirements in terms of weight, volume and especially environmental conditions (example: gravimetric power density of 115 kW/kg, for a 3 kV with 800 A molded circuit breaker for railway applications [115]). Thus, a research and development process for a functional aircraft circuit breaker is needed. The main parameters for this process are:

- Short-circuit current
- Inductive or capacitive behavior of the energy distribution grid
- Nominal current of the energy distribution grid
- Weight and volume
- Voltage level
- Environmental conditions

The high power requirements of the aircraft during climb make the usage of energy storage systems with high short circuit power unavoidable. This has to be considered during short-circuit and nominal current calculations. Furthermore, the cable design and routing will influence the complex impedance of the wiring harness which has to be considered in the failure calculation as well. The circuit breakers have to be weight- and volume-optimized for a reasonable use on an aircraft. With an increased grid voltage, the clearing distances of the circuit breaker have to be adjusted to meet the environmental conditions regarding altitude and temperature [116]. Additional parameters for the development and design are:

- Number of switching operations
- Contact- or on-state resistance
- Explosion protection
- Possible galvanic isolation
- Switching time
- EMC resistance

The number of switching operations which should be performed by the circuit breaker (nominal and short circuit) has to be defined. It is recommended that nominal switching operations should exceed 10,000 to lower the need for maintenance during the whole lifetime of the aircraft. To reduce weight of the circuit breaker, it may be possible to reduce the nominal operations, but also with increasing wear. Such circuit breakers have to be repetitive changed during more frequent maintenance periods. The number of operations for short circuit currents should exceed three operations to provide an additionally safety margin [117]. Short-circuits may

only occur under extreme conditions during emergencies. After such an extreme condition- a mandatory check and maintenance of the safety equipment should include a check and a potentially change of the circuit breaker.

Contact- or on-state resistance have to be as small as possible to reduce the losses of the circuit breakers and to establish an overall energy-efficient system. Furthermore, the reduction of these losses prevents unacceptable warming of the circuit breaker due to resistive losses.

Additionally, it may occur that components suited for application in explosion-protected areas have to be installed. This may be necessary near fuel or hydrogen supply to avoid dangerous scenarios. Hot-spots and electrical discharges are expected to enhance the risk of an explosion. Therefore, the circuit breaker should be specially developed to avoid an enhanced risk. However, a systematic assessment of the potential ignition sources is in any case necessary.

A galvanic separation of the contacts is needed in all high voltage grids, [118]. It is required to ensure the safety of crew and technicians during maintenance intervals.

The switching time has an influence on the possible short-circuit current, [119]. To reduce the occurring short-circuit current, the detection and the interruption has to be optimized. A fast switching process will reduce the stress within the distribution grid.

Finally, a circuit breaker which is not affected by electromagnetic interference during operation is mandatory [120]. Interference by inverters and atmospheric influences will occur during operation and is not allowed to affect the circuit breaker under all circumstances. Therefore, the circuit breaker has to be resistant against EMI. During its development process, it is inevitable to respect newest technical requirements regarding EMC optimization.

Depending on the topology of the energy distribution grid, a suitable failure detection hardware and software has to coordinate and control the switches, as proposed in [121]. The detection algorithm has to detect, characterize and localize the failure. With this information, a selective switching operation has to be triggered. Uncommon failures, which lead to blinding [122], [123] or tripping of multiple switches [124] of conventional circuit breakers, have to be avoided through this algorithm. This coordinated switching is of particular importance for the safe operation of the energy distribution grid and leads to the smallest possible interference of the aircraft. Actual control mechanisms limit the efficiency of the system. No suitable protection ultimately leads to higher weight in the equipment in order to establish the highest possible safety requirements which should be applied for energy distribution in an AEA.

B. POSSIBLE CIRCUIT BREAKER TECHNOLOGIES
In general, different circuit breaker concepts are applicable in an energy distribution grid of an aircraft. However, the abovementioned requirements should be discussed for different concepts in order to propose the best suitable circuit
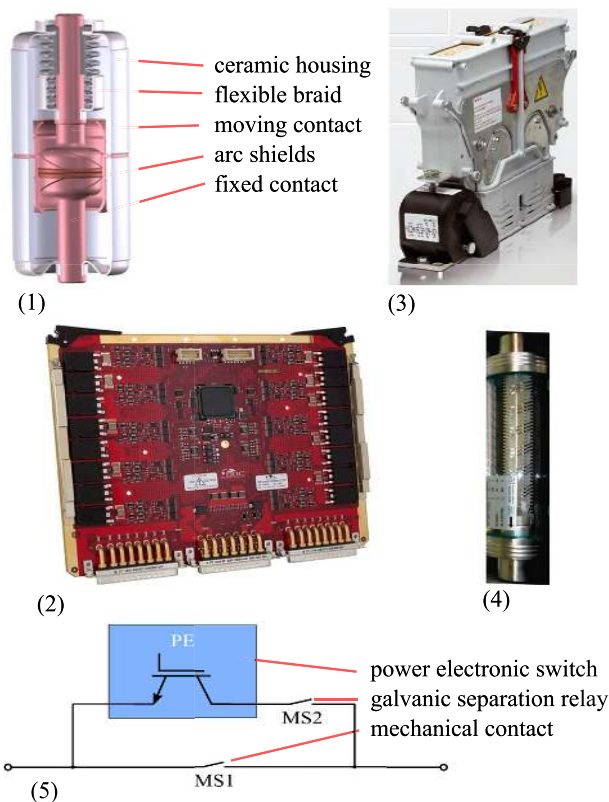
(1)

(3)

(2)

(4)

(5)

FIGURE 12. Examples for circuit breaker: (1) vacuum interrupter [125], (2) Solid state circuit breaker [126], (3) circuit breaker with arc chamber [115], (4) sketch of hybrid circuit breaker [127], (5) high voltage fuse [128].

breaker for this new application considering the high voltages, Fig. 12.

1) VACUUM INTERRUPTER
Typical circuit breakers in the medium voltage level are vacuum interrupters. Considering the special environmental conditions in an aircraft, they provide an excellent dielectric strength which is not affected by the reduced pressure in all operation heights. Furthermore, through hermetic encapsulation and low contact resistances in the area of several $\mu\Omega$, they provide advantages considering the explosion protection assessment of the system. Currents up to 63.5 kA at several 10 kV are switchable providing a galvanic separation. However, direct currents are not yet interruptible due to the missing repetitive current zero crossing. Additionally, the weight of these circuit breakers is enhanced due to the motor drives which are necessary to move the contact in the vacuum. However, for AC distribution systems with high voltages, this may be a technology which should be considered in a protection system assessment.

2) ELECTRONIC CIRCUIT BREAKER
Solid State Circuit Breakers (SSCB) or Solid State Power Controllers (SSPC) are the state of the art for energy distribution in aircrafts up to DC voltages of 270 V [120]. DC and AC voltages of variable frequencies are controllable

by these devices. Higher voltage levels are not available at the moment, however, in the near future, SSCB could be developed using new types of power semiconductors with higher blocking voltages. The sizing of the SSCB is in principal depending on the short-circuit calculation with respect to inductive loads and nominal current flow. Additionally to the power semiconductor and the control unit, an overvoltage protection is needed within the SSCB. For the further SSCB development, the occurring inductive loads should be considered as one main sizing parameter.

However, using this principle, no galvanic isolation is provided which is a disadvantage considering the personal safety. Furthermore, with the power semiconductors in the main path of the SSCB, the on-state resistance is increased compared to all mechanical circuit breakers. The increase compared to mechanical circuit breaker depends on the semiconductors. In a first approach an increase of three orders of magnitude is a first permissible generalisation. This leads to comparable high losses and the possible formation of hotspots on the circuit board, especially considering the high nominal currents during climb. A suitable cooling design is necessary which increases the weight of the SSCB significantly.

Principally, the SSCB is a low risk considering explosion protection, however, hotspots and surface charges still have to be considered in the risk assessment.

3) CIRCUIT BREAKER WITH ARC CHAMBER
Circuit breakers with arc chambers are available for different applications (for example, electrical vehicles, manufacturing facilities or rail applications). Applications for several MW switching capability are available and state of the art. The circuit breaker can securely provide this high switching power even with high voltages up to 3 kV, [115].

During the breaking process, a controlled arc is ignited and driven into the arc chamber (consisting of arc splitter blades or ceramic blades). The arc voltage rises above grid voltage level. As a result, the arc is extinguished within several milliseconds. Bidirectional DC as well as AC currents can be forced safely to zero, applying this principle. However, mechanical complex geometries are necessary which increases the weight of this circuit breaker technology. Furthermore, the weight increases even more for AEA application because of the special conditions in aircraft [116]. Here, the creeping and air distances of the contacts have to be increased due to the lower air pressure. The contact resistance can be kept low within several $\mu\Omega$, resulting in only few electrical losses. However, the explosion protection of the system has to be considered exhaustively because of the appearance of hot plasma and gases within the arc chamber during arc quenching. Depending on the location of operation, a capsulation of the circuit breaker can be necessary. In most cases, CB with arc chambers establishes a galvanic separation. The number of operations for nominal currents is limited to several thousand because of occurring erosion at the switching contacts.

Additionally, it shall be mentioned that circuit breakers with reduced weight are in principal possible and able to control high arc voltages but at the expense of switching operations due to the use of forced vaporizing polymers, [129].

4) HYBRID CIRCUIT BREAKER

A combination of an arc-based circuit breaker and power semiconductor has been described in many research and development projects in the last years [119], [127]. This type of switch unites advantages of both switching principles with reduced weight and volume requirements. Cooling systems to protect the power electronic equipment are not necessary but an overvoltage protection is mandatory. The cooling can be avoided, since the current during on-state is conducted by the electrical contacts with their low forward resistance. Complex and heavy arc chambers are avoided since the switch-off process is carried out by the power electronic part of the hybrid circuit breaker. The occurring contact erosion is strongly reduced in contrast to other switching principles; as a result, the service life of a hybrid switch is strongly extended.

Hybrid circuit breakers are realizable in different topologies, [119], [127], [130]–[132]. Using this switching principle leads to several different possibilities for galvanic separation, current capacity, dielectric strength, weight and volume.

5) FUSES

In principal, fuses provide a good switching performance with low volume and weight of the components. Furthermore, there are several possibilities to trigger fuses remotely, for example, by a failure detection algorithm [122]. However, the missing possibility to switch-on is in case of emergency in an aircraft is substantial.

6) CONCLUSION OF CIRCUIT BREAKER TECHNOLOGIES

The result of to the discussed circuit breaker principles have been summarized in Table 2. In this table, parameters which are beneficial for an application of this circuit breaker within an AEA are marked with "+" and even better with "++". Non-beneficial, but no parameters which exclude this technology, are marked with "o". Finally, parameters which prevent the application of this technology within an AEA are marked with "−".

The hybrid switch theoretically provides an acceptable trade-off for the regarded parameters. Some parameters here are dependent on the chosen circuit breaker topology as discussed below. However, the table is concluded for all switches as a first rough estimation, thus no actual circuit breaker in the assumed area of operation and for this application is available at the moment. For the hybrid switch, the values in the table were extrapolated, and assuming [127], they were measured for voltages up to 475 V, a time constant up to 3 ms and currents of up to 200 A. These values are derived from a model switch for scientific purposes and can be increased scientifically in industry products. However, voltages over 3 kV will need a different design lack of discrete IGBTs, thus

TABLE 2. Possible circuit breaker for AEAs.

	Vacuum CB	SSCB	CB with arc chamber	Hybrid CB	Fuse
Voltage level	++	+	+	+	+
Nominal current	++	o	++	++	+
Switching operations	o	++	o	+	-
DC operation	-	+	+	+	o
Galvanic isolation	++	-	+	+	+
Forward resistance	++	0	++	++	o
Explosion protection	++	+	o	+ / o	+
Weight	-	+	o	+ / o	++

a reliable assumption for this application is not possible at the moment.

C. HYBRID CIRCUIT BREAKER TOPOLOGIES

For further consideration, the hybrid switch will be discussed in terms of possible topologies. Different topologies can affect some decision criteria as marked in Table 2. At the moment, different possible topologies are under development. The different approaches can be sub-classified into:

1) Arc-free circuit breaker
2) Circuit breaker with reduced arc occurrence
3) Circuit breaker with optimized arc chamber

Every topology provides its own advantages and disadvantages during its operation within an AEA, which will be discussed below. However, every topology can be realized for bi-directional switching.

1) TOPOLOGY

Askan published in [132] an approach for circuit breakers up to 125 A at a voltage level of 380 V. This circuit breaker is suitable for suppressing short-circuit currents up to 20 kA. The possible maximum time constant for the switching process is not mentioned in this publication. The principal topology consists of, Fig. 13:

- Mechanical switches (MS)
- Auxiliary power electronic switches in the main path (APES)
- Power electronic switches in the switching part of the hybrid topology (MPES)

In the main branch of the switch topology, the MOSFET of the APES is chosen with low on-state resistance. The forward losses are mentioned with several 10 W, linearl extrapolated
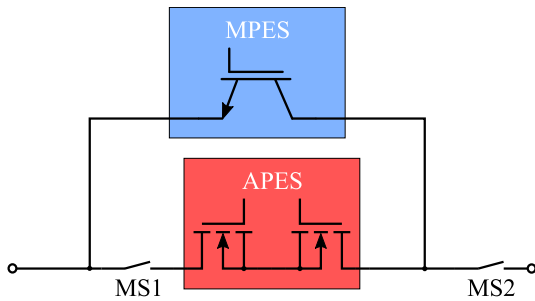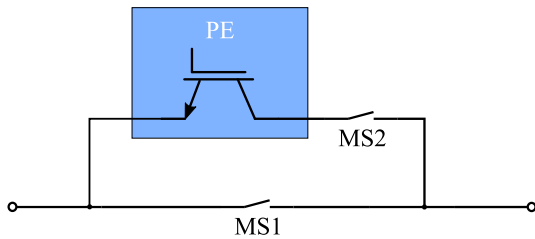
FIGURE 13. Hybrid switch topology 1.

FIGURE 14. Hybrid switch topology 2.

FIGURE 15. Hybrid switch topology 3.

to the assumed area of operation, leading to forward losses of several hundred watts.

During the switching process, the current commutates from the main branch to the switching branch with the MPES. This is where the switching process with the main power electronic takes place. After current zero, MS2 can be opened to achieve a galvanically separated state of the circuit breaker. One important advantage of this topology is the theoretically completely arc-free switching process by the APES in the main path. The explosion protection of this switching principle is superior for the regarded hybrid switch topologies, however, the MOSFET provides a significant barrier layer capacity. This will result in a large changing current when the mechanical switch is closed, which may cause a pre-strike arc. This has to be considered in an explosion protection assessment.

A disadvantage of this topology is that for the operation of the driver circuit, an external voltage supply for the APES and the MPES is necessary. Here redundancy for the use in an aircraft has to be considered in the development process. Furthermore, a failure of one part of the power electronic equipment leads to a complete failure of the whole device where the device will remain conductive; no fail-safe state is possible.

2) TOPOLOGY

Topology 2) of a hybrid switch is given in Fig. 14 and is published by Bösche *et al.* [127]. This approach was successfully demonstrated for voltages up to 475 V and currents of 200 A with a time constant of 3 ms. Topology 2) consists of:

- Mechanical switch in the main branch
- Power electronics for the switching process
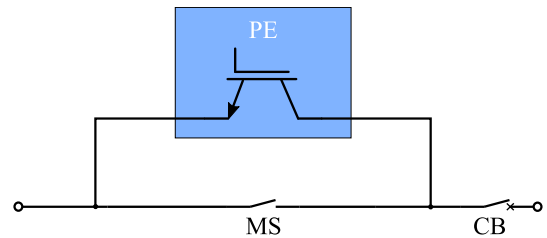- Mechanical switch for galvanic separation in the switching branch

In this topology, the Power Electronics (PE) is in parallel connection to a mechanical switch. During a switching process, MS1 opens and draws an arc. With an occurring arc voltage, the PE drive switches the PE on. The current commutates from the main branch onto the power electronics. The arc deionizes within a known time period [133]. With a sufficient dielectric strength of Mechanical Switch MS1, the power electronics is switched off. The current is suppressed to zero by a varistor within PE. For the following galvanic separation switch MS2 has to be opened afterwards.

An advantage of this topology is the simple construction of the device. With the intentionally arc formation the voltage supply for the driver circuit can be used from the arc voltage itself [127], [134]. Furthermore, the on-state resistance is small, thus only one mechanical contact with typical contact resistances of several micro ohms is conducting during switch-on.

A disadvantage of this topology is that the explosion protection is reduced, as an arc is necessary for the driver circuit. Furthermore, the contact erosion is not completely avoided through the arc in MS1. But in contrast to typical circuit breakers with arc chambers, the erosion is strongly decreased. Like Fig. 13, this switch has no fail safe, thus with a failure in the power electronics a switch-off is not possible anymore.

3) TOPOLOGY

The robustness possibility for a hybrid switch is given in Fig. 15 and consists of:

- Mechanical switch in the main branch
- Power electronics for the switching process
- Circuit breaker for fail-safe

The functionality of this switching topology is comparable to Fig. 14. Thus, after switch-off through the power electronics, a special designed circuit breaker establishes the galvanic separation, [127]. This provides the advantage that in the case of a failure of the power electronics, the circuit breaker will establish a fail-safe state. In contrast to conventional circuit breakers with arc chamber, this circuit breaker can be distinctly lighter, so that only one switching operation under load is necessary.

As in Fig. 14, the arc voltage can directly supply the driver.

Disadvantages are the slightly increased weight, and the doubled contact resistance, so that two switches in series connection are necessary.

However, every topology and switching technology has its own superior advantages. An assessment of the topology for

the given area of operation within the system is necessary. For a highly trustworthy operation of the power distribution, topology 3) is recommended. But this component has to be included into the maintenance periods. If an additional explosion protection is needed, the use of a completely molded hybrid switch should be considered.

IX. WIRING HARNESS

Currently, a direct current distribution with voltage levels up to ±270 V is used in MEAs [135]–[137]. To enable a technology change to AEAs an increase of the supply voltage is necessary in order to reduce the weight of the electrical power transmission system, [20], [138]. With the actual supply voltage, the equipment weight of the energy supply is too high for an application in the aviation, due to the occurring high nominal currents for the overall electrical demand of an AEA, e.g. Section VI.

The increase of the supply voltage up to several kilovolts is needed to achieve a weight-optimized distribution grid [139], [140]. The use of a higher supply voltage provides new opportunities considering electrical aircraft components, however, serious challenges have to be carefully solved in several preceding research projects.

On the one hand, new grid technologies are under development and have to be further developed and analyzed, [8], [140], [141]. Among others, load flow calculations, failure scenario assessment and failure current calculations have significant influence on these grid technologies. The grid design with its components has the significance of a key technology for the whole AEA.

On the other hand, distribution components, switchgear (Section VIII) and power transmission lines, have to be changed drastically to meet the requirements for the operation in the aviation [116], [142]. The main challenges for the transmission lines to make higher voltages available are among others:

- Arcing
- Partial discharge (Partial Discharge (PD))
- Surface charges
- Thermal management
- Conductor material

Arcing is a major risk during the operation of an aircraft [143], [144]. The risk and the potential damage increased significantly with the use of a DC supply voltage [145]. Publications point out that the use of aluminum conductors could increase the possible damage of an occurring arcing [143]. Thus, an appropriate choice of insulation material of the cables is needed [145], [146]. Furthermore, switchgears with fault arc detection and sufficient switching capability are essential for a safe operation of an AEA [147]. Especially for meshed DC-grids, further research is needed to ensure a safe operation [148]. The occurrence of PD in DC-systems is a known issue [149], [150]. The occurrence of PD within the wiring harness has to be excluded to increase the reliability of the insulation of the distribution cables and to
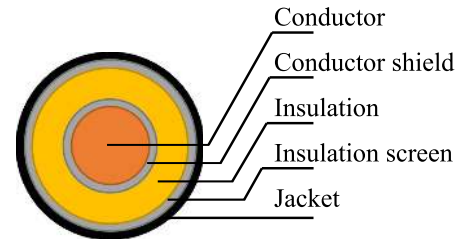
FIGURE 16. Possible cable structure for high voltage distribution for AEA.

minimize the risk of arcing [151]. However, due to the wiring praxis in electrical aircraft electrical field enhancements can be the consequence and lead to PD [152], [153]. Furthermore, high operating temperatures due to high distribution currents could lead to a faster aging of the cables and have to be tested in PD-tests before the cable design is selected [149], [154], [155]. Solutions to eliminate PDs could be developed in future research projects, like the use of screened cables [156] and new insulation materials which provide better PD resistance sheathes [157]. Surface charges of different insulation materials could lead to electrostatic discharges. Discharges with comparably low energy could ignite hydrogen which is a possible energy source of an AEA, e.g. Section VI. With regard to the lower ignition propensity a risk assessment with regard to explosion protection is needed for the use of any distribution cable within an AEA powered by a fuel cell.

The dimensioning of power cables is highly dependent on the temperature behaviour of the cable [158]. For the development of new types of cables especially designed for high power transmission on board of an aircraft, there are some physical limits regarding the temperature behaviour. In contrast to current cables, the calculation under full load is necessary to provide weight-optimized components. Current dimensioning regulations only calculate with partial load of the cables [142] Chapter 3.8.8.1.1. Physical limitations in cable development are:

- A strongly limited convection due to the lower air pressure (depending on the flight altitude)
- Heat conduction only at the connectors
- Possibly limited radiation losses due to thermal stability of insulation materials

The selection of the conductor material is discussed and assumed in several publications [139], [159]. For high transmission, powers aluminum is mainly preferred as conductor material due to the ratio of weight to power transmission [139]. However, apart from the fact that the calculation is based on the design for the traditional power transmission on board [139] and not on the not yet defined special case HVDC, there are restrictions by the Federal Aviation Administration (FAA) which limit the use of aluminum as conductor material [142]. Among others, these restrictions are:

- No approval of aluminum cables on engines
- No mounting on areas with severe vibrations

A principal cable structure is shown in Fig. 16:

Here, conductor shield and insulation screen fulfill the tasks of a field grading. The insulation material could be

classic materials like PTFE, ETFE, PI [145], maybe even materials adapted from HVDC transmission cables like XLPE [157] have to be considered, taking into account the abovementioned boundary conditions. The jacket serves as mechanical protection and consists of plastic materials like PVC.

In conclusion, there are many research projects ongoing which will enable us to design better and more reliable high-power transmission cables in the future. However, more research efforts especially for the aviation are needed to take the transmission voltage and transmission power to a new feasible level. Interesting studies with high potential are currently being carried out. They discuss and suggest different new technology solutions like superconductivity [160], selective protection of DC grids [121] and many more.

X. CONCLUSION AND OUTLOOK

The air transportation sector today produces a large amount of CO_2 emissions. Additionally, fossil energy resources are limited. Like in transportation on rail and on the road, new concepts are needed for air transportation. Approaches for sustainable air transport are based on synthetic fuels or electrochemical sources followed by consequent electrification. The first step towards more electrification are MEAs like Airbus A 380 and Boeing 787-8 Dreamliner with approximately 1 MVA electrical power at maximum. Here, the electrical power is generated by four generators of the conventional main engines. For future AEAs, hydrogen and batteries are suggested as the only energy sources which deliver electrical energy to an electrical power system of an aircraft.

The goal of this publication is the discussion about future electrical power systems for an AEA with a maximum power demand of 3.7 MW for short-range flights. Important electrical components in the power system are power converters, cables, and safety switches. Highest power density for all of these components is a must. Due to the high energy demand, the conventional AC distribution system has to be replaced by a DC system with an increased voltage level.

Fast-switching wide bandgap semiconductors, based on SiC and GaN, are a promising approach to follow the discussed path. Assuming two-level power electronic converters, 6.5 kV SiC semiconductors seem to be a viable solution to operate at a DC voltage of 3 kV($\pm$1.5 kV), while also allowing for a high switching frequency and therefore size reduction of passive components. Reliability and safety are still open issues. Gate oxide reliability and short-circuit capability are still under critical discussion. For high altitudes, also cosmic radiation has to be considered. Decreased reliability due to cosmic radiation is currently examined. However, especially wide bandgap devices promise an increased ruggedness to radiation compared with conventional Si switches. The demand for high voltage and high switching frequency devices for the application in AEA could further drive SiC semiconductor development and use. GaN devices are commercially available today with lower voltage ratings up to 650 V. A strong blocking voltage increase seems unlikely

during the next years. For the application in a 3 kV HVDC power system of an AEA, multilevel topologies like ANPC or MMC are needed. The higher number of used switches leads to increased complexity. Therefore, the application of GaN devices is most likely in smaller PoL and medium power converters far below 1 MW power. The reduction of passive component size is possible due to higher switching frequency but has to be balanced against EMI issues. The reliability of GaN is completely under investigation.

The need of a galvanic isolation in power electronic topologies is under discussion. At a first glance, non-isolated topologies like synchronous bidirectional converters promise lower weight. If the output voltage of the sources is in the range of the HVDC voltage level of 3 kV ($\pm$1.5 kV), this converter type delivers high efficiency. Due to the absence of a transformer, the effort for EMI filtering will increase in comparison to isolated converters. The EMI filtering complexity depends on several factors like switching frequency, modulation strategy, design of the circuit, magnetic component and cooling path. Investigations are required to get a concrete design.

The use of circuit breakers in an AEA is discussed with several different types which are rated in conclusion. The selection process of CBs is rather complex and has to consider different requirements like environmental conditions and aircraft standards, they influence the component parameters, such as short-circuit current and supply voltage. For a highly reliable operation of the power distribution system, a hybrid circuit breaker is a viable alternative to the current SSCBs, as they provide promising capabilities regarding galvanic isolation, gravimetric power density and supply voltage. The hybrid circuit breaker could be a key component to enable fully electrified aviation. The hybrid CB provides a good trade-off for the main requirements as given in Table 2. However, considering the current research and development effort, the area of operation of these CB will increase significantly in the next years. Furthermore, for the operation of hybrid switches in an AEA, several open questions have to be answered: dielectric restoration of the arc within the CB, the behavior of the dielectric strength within the CB, EMC, influence of cosmic radiation on the power semiconductors, thermal management in an environment of reduced air pressure and explosion protection. Additionally, the CB has to be included in the maintenance periods.

Concerning the wiring harness, many questions remain unanswered. Several important design parameters like altitude, grid structure, voltage level and nominal current level are unknown. Also, the behavior of the materials has to be investigated for the proposed cables, concerning arcing, partial discharge, surface charges, thermal management and conductor materials.

All the issues discussed will have to be examined in detail in the coming years. Many research efforts are currently in progress, and a promising solution should be available within the required time frame.

REFERENCES

[1] *Flightpath 2050: Europe's Vision for Aviation; Maintaining Global Leadership and Serving Society's Needs; Report of the High-Level Group on Aviation Research*, Eur. Commission, Publications Office Eur. Union, Luxembourg, U.K., 2011.

[2] S. Kelly and D. K. Kumar. *Jet Fuel Costs Could Rise From New Rules to Improve Air Quality*. Accessed: Nov. 11, 2019. [Online]. Available: https://uk.reuters.com/article/shipping-imo-jet-fuel/jet-fuel-costs-could-rise-from-new-rules-to-improve-air-quality-idUKL2N22X1N9

[3] International Air Transport Association. (2019). *Fuel Fact Sheet*. [Online]. Available: https://www.iata.org/contentassets/25e5377cf53c4e48bbaa49d252f3ab03/fact-sheet-fuel.pdf

[4] P. Wheeler and S. Bozhko, "The more electric aircraft: Technology and challenges.," *IEEE Electrific. Mag.*, vol. 2, no. 4, pp. 6–12, Dec. 2014.

[5] R. I. Jones, "The more electric aircraft: The past and the future?" in *Proc. IEE Colloquium. Electr. Mach. Syst. Electric Aircr.*, London, UK, Nov. 1999, p. 1.

[6] J.-K. Mueller, A. Bensmann, B. Bensmann, T. Fischer, T. Kadyk, G. Narjes, F. Kauth, B. Ponick, J. Seume, U. Krewer, R. Hanke-Rauschenbach, and A. Mertens, "Design considerations for the electrical power supply of future civil aircraft with active high-lift systems," *Energies*, vol. 11, no. 1, p. 179, 2018.

[7] M. Tariq, A. I. Maswood, C. J. Gajanayake, and A. K. Gupta, "Aircraft batteries: Current trend towards more electric aircraft," *IET Electr. Syst. Transp.*, vol. 7, no. 2, pp. 93–103, Jun. 2017.

[8] A. Lucken, J. Brombach, and D. Schulz, "Design and protection of a high voltage DC onboard grid with integrated fuel cell system on more electric aircraft," in *Proc. Electr. Syst. Aircr., Railway Ship Propuls.*, Bologna, Italy, Oct. 2010, pp. 1–6.

[9] T. Kadyk, C. Winnefeld, R. Hanke-Rauschenbach, and U. Krewer, "Analysis and design of fuel cell systems for aviation," *Energies*, vol. 11, no. 2, p. 375, 2018.

[10] J. Brombach, A. Lucken, B. Nya, M. Johannsen, and D. Schulz, "Comparison of different electrical HVDC-architectures for aircraft application," in *Proc. Electr. Syst. Aircr., Railway Ship Propuls.*, Bologna, Italy, Oct. 2012, pp. 1–6.

[11] C. Salb, S. Gül, C. Cuntz, Y. Monschauer, and J. Weishäupl, *Klimaschutz in Zahlen: Fakten, Trends und Impulse Deutscher Klimapolitik*. Frankfurt, Germany: BMU, Druck-und Verlagshaus Zarbock GmbH & Co. KG, 2018. Accessed: Oct. 15, 2019. [Online]. Available: https://www.bmu.de/fileadmin/Daten_BMU/Pools/Broschueren/klimaschutz_in_zahlen_2018_bf.pdf

[12] German Static Federal Office. *Kohlendioxidemissionen Im Verkehr Gegenüber 1990 Gestiegen*. Accessed: Oct. 15, 2019. [Online]. Available: https://www.destatis.de/Europa/DE/Thema/Umwelt-Energie/CO2_Sektoren.html

[13] European Parliament. *CO_2 Emissions From Cars: Facts and Figures*. Accessed: Oct. 15, 2019. [Online]. Available: https://www.europarl.europa.eu/news/en/headlines/society/20190313STO31218/co2-emissons-from-cars-facts-and-figures-infographics

[14] Air Transport Action Group. *Facts and Figures*. Accessed: Oct. 15, 2019. [Online]. Available: https://www.atag.org/facts-figures.html

[15] International Air Transport Association. (2018). *IATA Forecast Predicts 8.2 billion Air Travelers in 2037*. Accessed: Oct. 15, 2019. [Online]. Available: https://www.iata.org/pressroom/pr/Pages/2018-10-24-02.aspx

[16] German Association for the Environment and Nature Conservation. *Die Wahren Kosten Des Fliegens: Klimakiller Luftverkehr*. Accessed: Oct. 15, 2019. [Online]. Available: https://www.bund.net/themen/mobilitaet/infrastruktur/luftverkehr/co2-emissionen/?wc21726

[17] U.S. Energy Information Administratio. *Annual Energy Outlook 2019*. Accessed: Oct. 15, 2019. [Online]. Available: https://www.eia.gov/outlooks/aeo/pdf/aeo2019.pdf

[18] United Nations. (2015). *Paris Agreement*. Accessed: Oct. 15, 2019. [Online]. Available: https://unfccc.int/process-and-meetings/the-paris-agreement/the-paris-agreement

[19] Airbus. *A380: Unique Passenger Experience*. Accessed: Oct. 15, 2019. [Online]. Available: https://www.airbus.com/aircraft/passenger-aircraft/a380.html

[20] B. Sarlioglu and C. T. Morris, "More electric aircraft: Review, challenges, and opportunities for commercial transport aircraft," *IEEE Trans. Transport. Electrific.*, vol. 1, no. 1, pp. 54–64, Jun. 2015, doi: 10.1109/TTE.2015.2426499.

[21] Boeing. *Boeing 787, Dreamliner*. Accessed: Oct. 15, 2019. [Online]. Available: http://www.boeing.com/commercial/787/

[22] Airbus. *E-Fan X, A Giant Leap Towards Zero-Emission Flight*. Accessed: Oct. 15, 2019. [Online]. Available: https://www.airbus.com/innovation/future-technology/electric-flight/e-fan-x.html#objective

[23] V. Madonna, P. Giangrande, and M. Galea, "Electrical power generation in aircraft: Review, challenges, and opportunities," *IEEE Trans. Transport. Electrific.*, vol. 4, no. 3, pp. 646–659, Sep. 2018, doi: 10.1109/TTE.2018.2834142.

[24] Rolls Royce. *The E-Fan X Programme*. Accessed: Oct. 15, 2019. [Online]. Available: https://www.rolls-royce.com/media/our-stories/insights/2018/paul-stein-talks-about-e-fan-x.aspx

[25] J. Welstead and J. L. Felder, "Conceptual design of a single-aisle turbo-electric commercial transport with fuselage boundary layer ingestion," in *Proc. 54th AIAA Aerosp. Sci. Meeting*, Jan. 2016, p. 1027, doi: 10.2514/6.2016-1027.

[26] J. L. Kratz and G. L. Thomas, "Dynamic analysis of the STARC-ABL propulsion system," in *Proc. AIAA Propuls. Energy Forum*, Aug. 2019, p. 4182. [Online]. Available: https://arc.aiaa.org/doi/abs/10.2514/6.2019-4182

[27] K. V. Papathakis, K. J. Kloesel, Y. Lin, S. Clarke, J. J. Ediger, and S. Ginn, "Design and development of a 200-kW turbo-electric distributed propulsion testbed," in *Proc. 52nd AIAA/SAE/ASEE Joint Propuls. Conf. (Propuls. Energy)*, Jul. 2016, p. 17. [Online]. Available: https://ntrs.nasa.gov/search.jsp?R=20160009765

[28] M.-F. Liou, D. Gronstal, H. J. Kim, and M.-S. Liou, "Aerodynamic design of the hybrid wing body with nacelle: N3-X propulsion-airframe configuration," in *Proc. 34th AIAA Appl. Aerodyn. Conf.*, Jun. 2016, p. 3875. [Online]. Available: https://arc.aiaa.org/doi/10.2514/6.2016-3875

[29] M. J. Armstrong, M. Blackwelder, A. Bollman, C. Ross, A. Campbell, C. Jones, and P. Norman, "Architecture, voltage, and components for a turboelectric distributed propulsion electric grid," Nat. Aeronaut. Space Admin., Washington, DC, USA, Final Rep. NASA/CR-2015-218440, 2015, p. 270. [Online]. Available: https://ntrs.nasa.gov/archive/nasa/casi.ntrs.nasa.gov/20150014237.pdf

[30] J. J. Berton and W. J. Haller, "A noise and emissions assessment of the N3-X transport," in *Proc. 52nd Aerosp. Sci. Meeting*, Jan. 2014, pp. 1–22. [Online]. Available: https://ntrs.nasa.gov/archive/nasa/casi.ntrs.nasa.gov/20150014237.pdf

[31] X. Roboam, B. Sareni, and A. Andrade, "More electricity in the air: Toward optimized electrical networks embedded in more-electrical aircraft," *IEEE Ind. Electron. Mag.*, vol. 6, no. 4, pp. 6–17, Dec. 2012, doi: 10.1109/MIE.2012.2221355.

[32] M. Sinnett, "787 no-bleed systems: Saving fuel and enhancing operational efficiencies," Boeing AEROMAGAZINE, A Quarterly Publication, Seattle, WA, USA, Tech. Rep., 2014. [Online]. Available: http://www.boeing.com/commercial/aeromagazine/articles/qtr_4_07/index.html

[33] P. Wheeler, "Technology for the more and all electric aircraft of the future," in *Proc. IEEE Int. Conf. Automatica (ICA-ACCA)*, Oct. 2016, pp. 1–5, doi: 10.1109/ICA-ACCA.2016.7778519.

[34] A. Lücken, "Integration von brennstoffzellen in flugzeugbordnetze," Ph.D. dissertation, VDE Verlag GMBH, Helmut-Schmidt-Univ., Hamburg, Germany, 2014.

[35] Z. Dai, L. Wang, and S. Yang, "Fuel cell based auxiliary power unit in more electric aircraft," in *Proc. IEEE Transp. Electrific. Conf. Expo, Asia–Pacific (ITEC Asia–Pacific)*, Aug. 2017, pp. 1–6, doi: 10.1109/ITEC-AP.2017.8080851.

[36] S. Wu and Y. Li, "Fuel cell applications on more electrical aircraft," in *Proc. 17th Int. Conf. Electr. Mach. Syst. (ICEMS)*, Oct. 2014, pp. 198–201, doi: 10.1109/ICEMS.2014.7013481.

[37] N. Beck, T. Landa, A. Seitz, L. Boermans, Y. Liu, and R. Radespiel, "Drag reduction by laminar flow control," *Energies*, vol. 11, no. 1, p. 252, Jan. 2018.

[38] O. Meier and D. Scholz. (2010). *Estimation of Power Requirements for Electrical De-Icing Systems*. [Online]. Available: https://www.fzt.haw-hamburg.de/pers/Scholz/MOZART/MOZART_PUB_DLRK_10-08-31.pdf

[39] J. Herzog, "Electrification of the environmental control system," in *Proc. 25th Int. Congr. Aeronaut. Sci.*, 2006, pp. 1–4. [Online]. Available: http://icas.org/ICAS_ARCHIVE/ICAS2006/PAPERS/344.PDF

[40] D. Eugenio, G. Di Rito, R. Galatolo, and F. Schettini, "All-electric flight control system and landing gear system models for power assessment studies," in *Proc. 3AF/CEAS Conf. 'Greener Aviation, Clean Sky Breakthroughs Worldwide Status*, Bruxelles, Belgium, 2014.

[41] *Type-Certificate Data Sheet: Pratt & Whitney Canada PW150 Series*, Eur. Aviation Saf. Agency, Cologne, Germany, 2014.

[42] B. Jux, S. Foitzik, and M. Doppelbauer, "A standard mission profile for hybrid-electric regional aircraft based on Web flight data," in *Proc. IEEE Int. Conf. Power Electron., Drives Energy Syst. (PEDES)*, Chennai, India, Dec. 2018, pp. 1–6.

[43] Engineering ToolBox, *U.S. Standard Atmosphere*. Accessed: Nov. 22, 2019. [Online]. Available: https://www.engineeringtoolbox.com/standard-atmosphere-d_604.html

[44] F. Paschen, "Über die zum Funkenübergang in Luft, Wasserstoff und Kohlensäure bei verschiedenen Drücken erforderliche potentialdifferenz," *Ann. Phys.*, vol. 273, no. 5, pp. 69–96, 1889.

[45] NASA Langley Research Center. *Nowcast of Atmospheric Ionizing Radiation System: Current Dose Rates*. Accessed: Feb. 7, 2020. [Online]. Available: http://sol.spacenvironment.net/~nairas/Dose_Rates.html

[46] W. Friedberg and K. Copeland, *Ionizing Radiation in Earth's Atmosphere and in Space Near Earth*, Civil Aerosp. Med. Inst. Oklahoma City, Washington, DC, USA, May 2011.

[47] B. Tala-Ighil, J.-L. Trolet, H. Gualous, P. Mary, and S. Lefebvre, "Experimental and comparative study of gamma radiation effects on Si-IGBT and SiC-JFET," *Microelectron. Rel.*, vol. 55, nos. 9–10, pp. 1512–1516, Aug. 2015, doi: 10.1016/j.microrel.2015.06.136.

[48] K. Boomer, L. Scheik, and A. Hammoud. *Body of Knowledge (BOK): Gallium Nitride (GaN) Power Electronics for Space Applications*. Accessed: Jul. 7, 2020. [Online]. Available: https://nepp.nasa.gov/workshops/etw2019/talks/0619WED/1300%20-%20GaN%20BOK%20NEPP%20ETW%20Presentation7.pdf

[49] M. Zerarka, P. Austin, A. Bensoussan, F. Morancho, and A. Durier, "TCAD simulation of the single event effects in normally-off GaN transistors after heavy ion radiation," *IEEE Trans. Nucl. Sci.*, vol. 64, no. 8, pp. 2242–2249, Aug. 2017.

[50] A. Y. Polyakov, S. J. Pearton, P. Frenzer, F. Ren, L. Liu, and J. Kim, "Radiation effects in GaN materials and devices," *J. Mater. Chem. C*, vol. 1, no. 5, pp. 877–887, 2013.

[51] S. J. Pearton, R. Deist, F. Ren, L. Liu, A. Y. Polyakov, and J. Kim, "Review of radiation damage in GaN-based materials and devices," *J. Vac. Sci. Technol. A, Vac. Surf. Films*, vol. 31, no. 5, Sep. 2013, Art. no. 050801.

[52] C. Weiß, "Höhenstrahlungsresistenz von Silizium-Hochleistungsbauelementen," Ph.D. dissertation, Chair Tech. Electrophys., Technische Univ. München, Munich, Germany, 2015.

[53] *Measurement and Reporting of Alpha Particle and Terrestrial Cosmic Ray-Induced Soft Errors in Semiconductor Devices*, document JESD89A, 2006.

[54] C. Felgemacher, "Investigation of reliability aspects of power semiconductors in photovoltaic central inverters for sunbelt regions," Ph.D. dissertation, Dept. Elect. Power Supply Syst., Univ. Kassel, Kassel, Germany, 2018.

[55] A. Ionascut-Nedelcescu, C. Carlone, A. Houdayer, H. J. von Bardeleben, J.-L. Cantin, and S. Raymond, "Radiation hardness of gallium nitride," *IEEE Trans. Nucl. Sci.*, vol. 49, no. 6, pp. 2733–2738, Dec. 2002.

[56] J. Lefévre, J.-M. Costantini, S. Esnouf, and G. Petite, "Silicon threshold displacement energy determined by photoluminescence in electron-irradiated cubic silicon carbide," *J. Appl. Phys.*, vol. 105, no. 2, Jan. 2009, Art. no. 023520.

[57] H. Y. Xiao, F. Gao, X. T. Zu, and W. J. Weber, "Threshold displacement energy in GaN: *Ab initio* molecular dynamics study," *J. Appl. Phys.*, vol. 105, no. 12, 2009, Art. no. 123527.

[58] J. Nakashima, A. Fukumoto, Y. Obiraki, T. Oi, Y. Mitsui, H. Nakatake, Y. Toyoda, A. Nishizawa, K. Kawahara, S. Hino, H. Watanabe, T. Negishi, and S. Iura, "6.5-kV full-SiC power module (HV100) with SBD-embedded SiC-MOSFETs," in *Proc. PCIM Eur. Int. Exhib. Conf. Power Electron., Intell. Motion, Renew. Energy Energy Manage.*, Jun. 2018, pp. 441–447.

[59] M. Hiller, D. Krug, R. Sommer, and S. Rohner, "A new highly modular medium voltage converter topology for industrial drive applications," in *Proc. 13th Eur. Conf. Power Electron. Appl.*, Sep. 2009, pp. 1–10.

[60] J. Kucka, S. Lin, J. Friebe, and A. Mertens, "Quasi-two-level PWM-operated modular multilevel converter with non-linear branch inductors," in *Proc. 21st Eur. Conf. Power Electron. Appl. (EPE ECCE Europe)*, Genova, Italy, Sep. 2019, pp. 1–10.

[61] Y. Liu, A. Elham, P. Horst, and M. Hepperle, "Exploring vehicle level benefits of revolutionary technology progress via aircraft design and optimization," *Energies*, vol. 11, no. 1, p. 166, Jan. 2018.

[62] J. Hoelzen, Y. Liu, B. Bensmann, C. Winnefeld, A. Elham, J. Friedrichs, and R. Hanke-Rauschenbach, "Conceptual design of operation strategies for hybrid electric aircraft," *Energies*, vol. 11, no. 1, p. 217, Jan. 2018.

[63] Bundesverband WindEnergie. (Jun. 2018). *BWE-Hintergrundpapier, Redispatch und—Welche Rolle spielen die Erneuerbaren?* [Online]. Available: https://www.wind-energie.de/themen/netze/publikationen-netze/#c2394

[64] Roland Berger LTD. (Oct. 2017). *Aircraft Electrical Propulsion-the Next Chapter of Aviation?* [Online]. Available: https://www.rolandberger.com/en/Publications/New-developments-in-aircraft-electrical-propulsion.html

[65] P. Titscher, P. Schön, M. Horst, U. Krewer, and A. Kwade, "Increasing energy densities of sulfur cathodes using dispersing and calendering processes for lithium-sulfur batteries," *Energy Technol.*, vol. 6, no. 6, pp. 1139–1147, Jun. 2018.

[66] *Batteries, European Battery Cell R&I Workshop*, Eur. Battery Alliance, Eur. Commission, Brussels, Belgium, Jan. 2018.

[67] S. Hansen, S. Shree, G. Neubüser, J. Carstensen, L. Kienle, and R. Adelung, "Corset-like solid electrolyte interface for fast charging of silicon wire anodes," *J. Power Sources*, vol. 381, pp. 8–17, Mar. 2018.

[68] U.S Office of Energy Efficiency & Renewable Energy, Fuel Cell Technologies Office. *Hydrogen Storage*. Accessed: Oct. 20, 2019. [Online]. Available: https://www.energy.gov/eere/fuelcells/hydrogen-storage

[69] M. Warncke, S. Fahlbusch, and K. F. Hoffmann, "DC/DC-converter for fuel cell integration in more electric aircraft applications," in *Proc. 19th Eur. Conf. Power Electron. Appl. (EPE ECCE Eur.)*, Sep. 2017, pp. P.1–P.10, doi: 10.23919/EPE17ECCEEurope.2017.8099134.

[70] D. Zhang, J. He, and D. Pan, "A megawatt-scale medium-voltage high efficiency high power density 'SiC+Si' hybrid three-level ANPC inverter for aircraft hybrid-electric propulsion systems," *IEEE Trans. Ind. Appl.*, vol. 55, no. 6, pp. 5971–5980, Nov./Dec. 2019.

[71] R. Jansen, C. Bowman, A. Jankovsky, R. Dyson, and J. Felder, "Overview of NASA electrified aircraft propulsion (EAP) research for large subsonic transports," in *Proc. 53rd AIAA/SAE/ASEE Joint Propuls. Conf.*, Jul. 2017, p. 4701.

[72] X. She, A. Q. Huang, O. Lucia, and B. Ozpineci, "Review of silicon carbide power devices and their applications," *IEEE Trans. Ind. Electron.*, vol. 64, no. 10, pp. 8193–8205, Oct. 2017, doi: 10.1109/TIE.2017.2652401.

[73] S. T. Pantelides *et al.*, "Si/SiO$_2$ and SiC/SiO$_2$ interfaces for MOSFETs—Challenges and advances," *Mater. Sci. Forum*, vols. 527–529, pp. 935–948, Oct. 2006, doi: 10.4028/www.scientific.net/MSF.527-529.935.

[74] M. A. Fraga, M. Bosi, and M. Negri, "Silicon carbide in microsystem technology-thin film versus bulk material," in *Advanced Silicon Carbide Devices and Processing*. London, U.K.: InTechopen, Sep. 2015, doi: 10.5772/60970.

[75] Cree Inc. *Cree to Invest $1 Billion to Expand Silicon Carbide Capacity*. Accessed: May 2, 2020. [Online]. Available: https://www.cree.com/news-events/news/article/cree-to-invest-1-billion-to-expand-silicon-carbide-capacity

[76] T. Sakaguchi, M. Aketa, T. Nakamura, M. Nakanishi, and M. Rahimo, "Characterization of 3.3 kV and 6.5 kV SiC MOSFETs," in *Proc. PCIM Eur. Int. Exhib. Conf. Power Electron., Intell. Motion, Renew. Energy Energy Manage.*, Jul. 2017, pp. 39–43.

[77] S. Sabri, E. Van Brunt, A. Barkley, B. Hull, M. O'Loughlin, A. Burk, S. Allen, and J. Palmour, "New generation 6.5 kV SiC power MOSFET," in *Proc. IEEE 5th Workshop Wide Bandgap Power Devices Appl. (WiPDA)*, Oct. 2017, pp. 246–250, doi: 10.1109/WiPDA.2017.8170555.

[78] V. Pala, E. V. Brunt, L. Cheng, M. O'Loughlin, J. Richmond, A. Burk, S. T. Allen, D. Grider, J. W. Palmour, and C. J. Scozzie, "10 kV and 15 kV silicon carbide power MOSFETs for next-generation energy conversion and transmission systems," in *Proc. IEEE Energy Convers. Congr. Exposit. (ECCE)*, Sep. 2014, pp. 449–454, doi: 10.1109/ECCE.2014.6953428.

[79] J. Thoma, B. Volzer, D. Kranzer, D. Derix, and A. Hensel, "Design and commissioning of a 10 kV three-phase transformerless inverter with 15 kV silicon carbide MOSFETs," in *Proc. 20th Eur. Conf. Power Electron. Appl. (EPE ECCE Eur.)*, Sep. 2018, pp. P.1–P.7.

[80] S. Harada, Y. Kobayashi, K. Ariyoshi, T. Kojima, J. Senzaki, Y. Tanaka, and H. Okumura, "3.3-kV-Class 4H-SiC MeV-implanted UMOSFET with reduced gate oxide field," *IEEE Electron Device Lett.*, vol. 37, no. 3, pp. 314–316, Mar. 2016, doi: 10.1109/LED.2016.2520464.

[81] P. Beckedahl, M. Spang, and O. Tamm, "Breakthrough into the third dimension—Sintered multi layer flex for ultra low inductance power modules," in *Proc. 8th Int. Conf. Integr. Power Electron. (CIPS)*, Mar. 2014, pp. 1–5.

[82] R. Mitova, R. Ghosh, U. Mhaskar, D. Klikic, M.-X. Wang, and A. Dentella, "Investigations of 600-V GaN HEMT and GaN diode for power converter applications," *IEEE Trans. Power Electron.*, vol. 29, no. 5, pp. 2441–2452, May 2014.

[83] P. Schulting, C. Winter, and R. W. De Doncker, "Design of a high-frequency dual-active bridge converter with GaN devices for an output power of 3.7 kW," in *Proc. Int. Power Electron. Conf. (IPEC-Niigata-ECCE Asia)*, Niigata, Japan, May 2018, pp. 388–395.

[84] H. Beiranvand, E. Rokrok, and M. Liserre, "Comparative study of heatsink volume and weight optimization in SST DAB cells employing GaN, SiC-MOSFET and Si-IGBT switches," in *Proc. 10th Int. Power Electron., Drive Syst. Technol. Conf. (PEDSTC)*, Shiraz, Iran, Feb. 2019, pp. 297–302.

[85] H. Amano, "The 2018 GaN power electronics roadmap," *J. Phys. D, Appl. Phys.*, vol. 51, no. 16, 2018, Art. no. 163001.

[86] K. J. Chen, O. Häberlen, A. Lidow, C. lin Tsai, T. Ueda, Y. Uemoto, and Y. Wu, "GaN-on-Si power technology: Devices and applications," *IEEE Trans. Electron Devices*, vol. 64, no. 3, pp. 779–795, Mar. 2017.

[87] H. Wang, M. Liserre, F. Blaabjerg, P. de Place Rimmen, J. B. Jacobsen, T. Kvisgaard, and J. Landkildehus, "Transitioning to physics-of-failure as a reliability driver in power electronics," *IEEE J. Emerg. Sel. Topics Power Electron.*, vol. 2, no. 1, pp. 97–114, Mar. 2014, doi: 10.1109/JESTPE.2013.2290282.

[88] R. Siemieniec, D. Peters, R. Esteve, W. Bergner, D. Kuck, T. Aichinger, T. Basler, and B. Zippelius, "A SiC trench MOSFET concept offering improved channel mobility and high reliability," in *Proc. 19th Eur. Conf. Power Electron. Appl. (EPE ECCE Eur.)*, Sep. 2017, pp. P.1–P.13, doi: 10.23919/EPE17ECCEEurope.2017.8098928.

[89] K. P. Cheung, "SiC power MOSFET gate oxide breakdown reliability—Current status," in *Proc. IEEE Int. Rel. Phys. Symp. (IRPS)*, Mar. 2018, pp. 2B.3-1–2B.3-5, doi: 10.1109/IRPS.2018.8353545.

[90] C.-T. Yen, H. Y. Lee, C. C. Hung, C. Y. Lee, L. S. Lee, F. J. Hsu, and K. T. Chu, "Oxide breakdown reliability of SiC MOSFET," in *Proc. IEEE Workshop Wide Bandgap Power Devices Appl. Asia (WiPDA Asia)*, May 2019, pp. 1–3, doi: 10.1109/WiPDAAsia.2019.8760324.

[91] F. Li, P. Mawby, Q. Song, A. Perez-Tomas, V. Shah, Y. Sharma, D. Hamilton, C. Fisher, P. Gammon, and M. Jennings, "A first evaluation of thick oxide 3C-SiC MOS capacitors reliability," *IEEE Trans. Electron Devices*, vol. 67, no. 1, pp. 237–242, Jan. 2020, doi: 10.1109/TED.2019.2954911.

[92] D. Peters, T. Aichinger, T. Basler, G. Rescher, K. Puschkarsky, and H. Reisinger, "Investigation of threshold voltage stability of SiC MOSFETs," in *Proc. IEEE 30th Int. Symp. Power Semiconductor Devices (ICs ISPSD)*, May 2018, pp. 40–43, doi: 10.1109/ISPSD.2018.8393597.

[93] J. Sun, H. Xu, X. Wu, S. Yang, Q. Guo, and K. Sheng, "Short circuit capability and high temperature channel mobility of SiC MOSFETs," in *Proc. 29th Int. Symp. Power Semiconductor Devices (IC's ISPSD)*, May 2017, pp. 399–402, doi: 10.23919/ISPSD.2017.7988988.

[94] S. G. Khalil, S. Hardikar, S. Sack, E. Persson, M. Imam, and T. McDonald, "HV GaN reliability and status," in *Proc. IEEE 3rd Workshop Wide Bandgap Power Devices Appl. (WiPDA)*, Blacksburg, VA, USA, Nov. 2015, pp. 21–23.

[95] A. Lidow, R. Strittmatter, C. Zhou, and Y. Ma, "Enhancement mode gallium nitride transistor reliability," in *Proc. IEEE Int. Rel. Phys. Symp.*, Atlanta, GA, USA, Apr. 2015, pp. 269–273.

[96] K.-Y. Roy Wong *et al.*, "A next generation CMOS-compatible GaN-on-Si transistors for high efficiency energy systems," in *IEDM Tech. Dig.*, Washington, DC, USA, Dec. 2015, pp. 9.5.1–9.5.4.

[97] L. Cao, Q. Guo, and K. Sheng, "Comparative evaluation of the short circuit capability of SiC planar and trench power MOSFET," in *Proc. IEEE 2nd Int. Electr. Energy Conf. (CIEEC)*, Nov. 2018, pp. 653–656, doi: 10.1109/CIEEC.2018.8745774.

[98] M. Landel, C. Gautier, D. Labrousse, and S. Lefebvre, "[131] experimental study of the short-circuit robustness of 600 V E-mode GaN transistors," *Microelectron. Rel.*, vol. 64, pp. 560–565, Sep. 2016.

[99] H. Li, X. Li, X. Wang, X. Lyu, H. Cai, Y. M. Alsmadi, L. Liu, S. Bala, and J. Wang, "Robustness of 650-V enhancement-mode GaN HEMTs under various short-circuit conditions," *IEEE Trans. Ind. Appl.*, vol. 55, no. 2, pp. 1807–1816, Mar. 2019.

[100] X. Huang, D. Y. Lee, V. Bondarenko, A. Baker, D. C. Sheridan, A. Q. Huang, and B. J. Baliga, "Experimental study of 650 V AlGaN/GaN HEMT short-circuit safe operating area (SCSOA)," in *Proc. IEEE 26th Int. Symp. Power Semiconductor Devices (IC's ISPSD)*, Waikoloa, HI, USA, Jun. 2014, pp. 273–276.

[101] C. Weiss, G. Wachutka, A. Hartl, F. Hille, and F. Pfirsch, "Predictive physical model of cosmic-radiation-induced failures of power devices," in *Proc. 15th Int. Power Electron. Motion Control Conf. (EPE/PEMC)*, Sep. 2012, pp. LS2e.3-1–LS2e.3-5, doi: 10.1109/EPEPEMC.2012.6397423.

[102] R. A. Prado and C. N. L. Gajo, "Power semiconductor failures due to cosmic rays," in *Proc. Brazilian Power Electron. Conf. (COBEP)*, Nov. 2017, pp. 1–6, doi: 10.1109/COBEP.2017.8257437.

[103] O. Kreutzer, M. Billmann, M. Maerz, and A. Lange, "Non-isolating DC/DC converter for a fuel cell powered aircraft," in *Proc. Int. Conf. Electr. Syst. Aircr., Railway, Ship Propuls. Road Vehicles Int. Transp. Electrific. Conf. (ESARS-ITEC)*, Feb. 2017, pp. 1–6, doi: 10.1109/ESARS-ITEC.2016.7841372.

[104] M. Mu, F. C. Lee, Y. Jiao, and S. Lu, "Analysis and design of coupled inductor for interleaved multiphase three-level DC-DC converters," in *Proc. IEEE Appl. Power Electron. Conf. Exposit. (APEC)*, Mar. 2015, pp. 2999–3006, doi: 10.1109/APEC.2015.7104779.

[105] N. Langmaack, G. Tareilus, and M. Henke, "SiC boost converter with high power density for a battery electric sports car," in *Proc. Hybrid Symp.* Lake Forest, IL, USA: Brunswick, 2014, pp. 7–8.

[106] B. Nya, J. Brombach, and D. Schulz, *Weight Evaluation of Cabin Power Architecture on Smaller Civil Aircrafts*. Aachen, Germany: Shaker, 2011.

[107] Z. Liao, Y. Lei, and R. C. N. Pilawa-Podgurski, "A GaN-based flying-capacitor multilevel boost converter for high step-up conversion," in *Proc. IEEE Energy Convers. Congr. Exposit. (ECCE)*, Milwaukee, WI, USA, Sep. 2016, pp. 1–7.

[108] Y.-F. Wu, "Paralleling high-speed GaN power HEMTs for quadrupled power output," in *Proc. 28th Annu. IEEE Appl. Power Electron. Conf. Exposit. (APEC)*, Long Beach, CA, USA, Mar. 2013, pp. 211–214.

[109] A. Mertens and J. Kucka, "Quasi two-level PWM operation of an MMC phase leg with reduced module capacitance," *IEEE Trans. Power Electron.*, vol. 31, no. 10, pp. 6765–6769, Oct. 2016.

[110] A. Rodriguez, A. Vázquez, D. G. Lamar, M. M. Hernando, and J. Sebastián, "Different purpose design strategies and techniques to improve the performance of a dual active bridge with phase-shift control," *IEEE Trans. Power Electron.*, vol. 30, no. 2, pp. 790–804, Feb. 2015, doi: 10.1109/TPEL.2014.2309853.

[111] B. Zhao, Q. Song, W. Liu, and Y. Sun, "Overview of dual-active-bridge isolated bidirectional DC–DC converter for high-frequency-link power-conversion system," *IEEE Trans. Power Electron.*, vol. 29, no. 8, pp. 4091–4106, Aug. 2014, doi: 10.1109/TPEL.2013.2289913.

[112] T. Lagier, L. Chedot, F. W. L. Ghossein, B. Lefebvre, P. Dworakowski, M. Mermet-Guyennet, and C. Buttay, "A 100 kW 1.2 kV 20 kHz DC-DC converter prototype based on the dual active bridge topology," in *Proc. IEEE Int. Conf. Ind. Technol. (ICIT)*, Feb. 2018, pp. 559–564, doi: 10.1109/ICIT.2018.8352238.

[113] T. Schobre, K. Siebke, and R. Mallwitz, "Design of a GaN based CLLC converter with synchronous rectification for on-board vehicle charger," in *Proc. PCIM Eur. Int. Exhib. Conf. Power Electron., Intell. Motion, Renew. Energy Energy Manage.*, Jul. 2019, pp. 1158–1162.

[114] K. Siebke and R. Mallwitz, "Operation mode analysis of the CLLC resonant converter," in *Proc. IEEE 13th Int. Conf. Compat., Power Electron. Power Eng. (CPE-POWERENG)*, Apr. 2019, pp. 1–6, doi: 10.1109/CPE.2019.8862405.

[115] Schaltbau GmbH, Muenchen, Germany. *03 Schuetze CT1115/04, CT1130/04 CT1115/08, CT1130/08*. Accessed: Feb. 4, 2020. [Online]. Available: https://www.schaltbau.com/media/c20/verb:_;de.pdf

[116] *Enviromental Conditions and Test Procedures for Airborne Equipment*, document EUROCAE ED-14F, 2008.

[117] *Circuit Breakers for Equipment (CBE)*, Standard IEC 60934, 2019.

[118] *Operation of Electrical Installations—Part 1: General Requirements*, Standard EN 50110-1, 2013.

[119] K. Askan, M. Bartonek, and F. Stueckler, "Bidirectional switch based on silicon high voltage superjunction MOSFETs and TVS diode used in low voltage DC SSCB," in *Proc. PCIM Eur. Int. Exhib. Conf. Power Electron., Intell. Motion, Renew. Energy Energy Manage.*, Nuremberg, Germany, 2019, pp. 1–8.

[120] D. Izquierdo, A. Barrado, C. Raga, M. Sanz, P. Zumel, and A. Lazaro, "Protection devices for aircraft electrical power distribution systems: A survey," in *Proc. 34th Annu. Conf. IEEE Ind. Electron.*, Orlando, FL, USA, Nov. 2008, pp. 903–908, doi: 10.1109/IECON.2008.4758073.

[121] C. Klosinski, P. Ross, N. Hemdan, M. Kurrat, F. Gerdinand, J. Meisner, S. Passon, and A. Heinrich, "Modular protection system for fault detection and selective fault clearing in DC microgrids," *J. Eng.*, vol. 2018, no. 15, pp. 1321–1325, Oct. 2018, doi: 10.1049/joe.2018.0193.

[122] H. Bessei and F. Glinka, "Smart fuses for smart grids," in *Proc. 10th Int. Conf. Electr. Fuses Appl.*, Dresden, Germany, Sep. 2015, pp. 2–5.

[123] M. Igel, M. Ames, F. Glinka, T. Wippenbeck, and P. Erlinghagen, "A generic model for fuses to calculate the transients in low-voltage power networks," in *Proc. 10th Int. Conf. Electric Fuses Appl.*, Dresden, Germany, Sep. 2015, p. 2.

[124] J. Niewind, N. G. A. Hemdan, C. Klosinski, D. Bösche, M. Kurrat, F. Gerdinand, J. Meisner, and S. Passon, "Operation and protection of 380 V DC distribution systems," in *Proc. IEEE Manchester PowerTech*, Manchester, U.K., Jun. 2017, pp. 1–6, doi: 10.1109/PTC.2017.7981063.

[125] L. T. Falkingham, "Vacuum switchgear; past, present, and future," in *Proc. 5th Int. Conf. Electr. Power Equip.-Switching Technol. (ICEPE-ST)*, Kitakyushu, Japan, Oct. 2019, pp. 788–793, doi: 10.1109/ICEPE-ST.2019.8928778.

[126] C E Howard, Nashville, TN, USA. (Jan. 12, 2016). *DDC debuts AC Solid-State Power Controller for Aircraft*. Accessed: Feb. 6, 2020. [Online]. Available: https://www.intelligent-aerospace.com/avionics/article/16538706/ddc-debuts-ac-solidstate-power-controller-for-aircraft

[127] D. Bosche, E.-D. Wilkening, H. Kopf, and M. Kurrat, "Hybrid DC circuit breaker feasibility study," *IEEE Trans. Compon., Packag., Manuf. Technol.*, vol. 7, no. 3, pp. 354–362, Mar. 2017, doi: 10.1109/TCPMT.2016.2613579.

[128] H. Kolwnatzky, "Highest level of professional training on circuit protection," in *Proc. 10th Int. Conf. Electr. Fuses Appl.*, Dresden, Germany, Sep. 2015, p. 5.

[129] T. Schrank, E.-D. Wilkening, and M. Kurrat, "Investigation of breaking performance of various arcing chambermaterials at DC voltage," in *Proc. 21st Albert-Keil-Kontaktseminar*, Karlsruhe, Germany, Sep. 2011, p. 2.

[130] J.-M. Meyer and A. Rufer, "A DC hybrid circuit breaker with ultra-fast contact opening and integrated gate-commutated thyristors (IGCTs)," *IEEE Trans. Power Del.*, vol. 21, no. 2, pp. 646–651, Apr. 2006, doi: 10.1109/TPWRD.2006.870981.

[131] L. Li, Z. Bi-de, F. Chun-en, L. Wei, R. Xiao, and D. Tishuai, "Researches on interruption characteristics of a hybrid HVDC circuit breaker," in *Proc. 4th Int. Conf. Electric Power Equip.-Switching Technol. (ICEPE-ST)*, Xi'an, China, Oct. 2017, pp. 448–451, doi: 10.1109/ICEPE-ST.2017.8188874.

[132] K. Askan, M. Bartonek, and K. Weichselbaum, "Power module for low voltage DC hybrid circuit breaker," in *Proc. 3rd IEEE ICDCM Int. Conf. DC Microgrids*, Matsue, Japan, May 2019, pp. 1–8.

[133] D. Bösche, M. Alija, M. Hilbert, and M. Kurrat, "Investigating of the recovery behaviour of a small switching gap after current interuption," *PLASMA Phys. Technol.*, vol. 4, no. 2, pp. 165–168, 2017.

[134] D. Bösche and E. Wilkening, "Method and voltage multiplier for converting an input voltage, and isolating circuit," EU Patent WO 162 133, Sep. 13, 2018.

[135] I. Christou, A. Nelms, M. Husband, and I. Cotton, "Choice of optimal voltage for more electric aircraft wiring systems," *IET Electr. Syst. Transp.*, vol. 1, no. 1, pp. 24–30, Mar. 2011, doi: 10.1049/iet-est.2010.0021.

[136] L. Setlak and R. Kowalik, "Comparative analysis and simulation of selected components of modern on-board autonomous power systems (ASE) of modern aircraft in line with the concept of MEA/AEA," in *Proc. World Congr. Eng. Comput. Sci.*, San Francisco, CA, USA, 2016, p. 1.

[137] L. Setlak and R. Kowalik, "Evaluation of the VSC-HVDC system performance in accordance with the more electric aircraft concept," in *Proc. 19th Int. Scientific Conf. Electric Power Eng. (EPE)*, Brno, Czech Republic, May 2018, pp. 1–6, doi: 10.1109/EPE.2018.8396043.

[138] P. Thalin, *Fundamentals of Electric Aircraft*. Warrendale, PA, USA: SAE International, 2019.

[139] S. Stückl, "Methods for the design and evaluation of future aircraft concepts utilizing electric propulsion systems," Ph.D. dissertation, Fakultät für Maschinenwesen, Technischen Univ. München, München, Germany, 2015.

[140] C. E. Jones, P. J. Norman, S. J. Galloway, M. J. Armstrong, and A. M. Bollman, "Comparison of candidate architectures for future distributed propulsion aircraft," *IEEE Trans. Appl. Supercond.*, vol. 26, no. 6, pp. 1–9, Sep. 2016, doi: 10.1109/TASC.2016.2530696.

[141] Y. Ji, "Model-based design and integration of the power network in more electric aircraft," Ph.D. dissertation, Fakultät für Maschinenwesen, Technischen Univ. München, München, Germany, 2016.

[142] *Wiring Aerospace Vehicle*, Standard AS50881, 2006.

[143] A. Gleizes, "The problem of electric arcs in aeronautics," in *Proc. 18th Symp. Phys. Switching Arc*, Brno, Czech Republic, 2013, p. 27.

[144] H. El Bayda, F. Valensi, M. Masquere, and A. Gleizes, "Energy losses from an arc tracking in aeronautic cables in DC circuits," *IEEE Trans. Dielectrics Electr. Insul.*, vol. 20, no. 1, pp. 19–27, Feb. 2013, doi: 10.1109/TDEI.2013.6451337.

[145] F. Dricot and H. J. Reher, "Survey of arc tracking on aerospace cables and wires," *IEEE Trans. Dielectrics Electr. Insul.*, vol. 1, no. 5, pp. 896–903, Oct. 1994, doi: 10.1109/94.326657.

[146] P. Meckler, "Simulation of AC Arc faults in aircraft electrical networks critical loads—Critical ignition energies," *SAE Trans.*, vol. 112, no. 1, pp. 584–589, 2003.

[147] C. Strobl and P. Meckler, "Basic experiments for detecting arc faults in DC aircraft networks," in *Proc. 24th Int. Conf. Electr. Contacts*, Saint-Malo, France, Jun. 2008, pp. 353–358.

[148] C. Strobl, H. Köpf, R. Mehl, L. Ott, J. Kaiser, K. Gosses, M. Schäfer, and R. Rabenstein, "Safety concepts and circuit protection for LVDC-grids in datacenters and in telecommunications," in *Proc. IEEE Int. Telecommun. Energy Conf. (INTELEC)*, Turin, Italy, Oct. 2018, pp. 1–6, doi: 10.1109/INTLEC.2018.8612360.

[149] N. Hill, M. Hilbert, and M. Kurrat, "Partial discharge testing for low voltage switchgear at high temperatures," in *Proc. IEEE Holm Conf. Electr. Contacts*, Milwaukee, WI, USA, Sep. 2019, pp. 1–5, doi: 10.1109/HOLM.2019.8923693.

[150] P. Romano, R. Candela, A. Imburgia, G. Presti, E. R. Sanseverino, and F. Viola, "A new technique for partial discharges measurement under DC periodic stress," in *Proc. IEEE Conf. Electr. Insul. Dielectric Phenomenon (CEIDP)*, Fort Worth, TX, USA, Oct. 2017, pp. 303–306, doi: 10.1109/CEIDP.2017.8257614.

[151] I. Cotton, A. Nelms, and M. Husband, "Higher voltage aircraft power systems," *IEEE Aerosp. Electron. Syst. Mag.*, vol. 23, no. 2, pp. 25–32, Feb. 2008., doi: 10.1109/MAES.2008.4460728.

[152] W. Xin, R. Mahmoudi, and C. E. Lents, "A study of partial discharge in high voltage DC distribution systems for hybrid electric aircraft," in *Proc. AIAA/IEEE Electr. Aircr. Technol. Symp. (EATS)*, Cincinnati, OH, USA, Jul. 2018, pp. 1–9.

[153] F. Alrumayan, I. Cotton, and A. Nelms, "Partial discharge testing of aerospace electrical systems," *IEEE Trans. Aerosp. Electron. Syst.*, vol. 46, no. 2, pp. 848–863, Apr. 2010, doi: 10.1109/TAES.2010.5461661.

[154] C. Emersic, R. Lowndes, I. Cotton, S. Rowland, and R. Freer, "The effects of pressure and temperature on partial discharge degradation of silicone conformai coatings," *IEEE Trans. Dielectrics Electr. Insul.*, vol. 24, no. 5, pp. 2986–2994, Oct. 2017, doi: 10.1109/TDEI.2017.006466.

[155] M. Karadjian, N. Imbert, C. Munier, M. Kirkpatrick, and E. Odic, "Partial discharge detection in an aeronautical power cable," in *Proc. AIAA/IEEE Electric Aircr. Technol. Symp.*, Cincinnati, OH, USA, Jul. 2018, pp. 1–9.

[156] C. Emersic, I. Cotton, and S. Smith, "High voltage systems—Challenges for future aircraft," presented at the Hybrid-Electr. Electr. Aircr.-Researching Challenges Introduction, London, U.K., May 30, 2017.

[157] D. Fabiani, G. C. Montanari, A. Cavallini, A. Saccani, and M. Toselli, "Nanostructured-coated XLPE showing improved electrical properties: Partial discharge resistance and space charge accumulation," in *Proc. Int. Symp. Electr. Insulating Mater.*, Kyoto, Japan, Sep. 2011, pp. 16–19, doi: 10.1109/ISEIM.2011.6826265.

[158] G. J. Anders, *Rating of Electric Power Cables in Unfavourable Thermal Environment*. Hoboken, NJ, USA: Wiley, 2005.

[159] S. H. Teichel, M. Dörbaum, O. Misir, A. Merkert, A. Mertens, J. R. Seume, and B. Ponick, "Design considerations for the components of electrically powered active high-lift systems in civil aircraft," *CEAS Aeronaut. J.*, vol. 6, no. 1, pp. 49–67, Mar. 2015, doi: 10.1007/s13272-014-0124-1.

[160] J. Rivenc, G. Peres, F. Berg, L. Prisse, P. Rostek, D. Melyukov, V. Amelichev, and S. Samoilenkov, "An evaluation of high temperature superconducting power cables for airborne application," in *Proc. AIAA/IEEE Electric Aircr. Technol. Symp.*, Cincinnati, OH, USA, Jul. 2018, pp. 1–21.

HENDRIK SCHEFER was born in Heide, Germany, in 1991. He received the B.Eng. degree from the Flensburg University of Applied Sciences, in 2016, the master's degree from the Institute for Electrical Machines, Traction and Drives, TU Braunschweig, in 2018. He is currently pursuing the Ph.D. degree with the Institute for Electrical Machines, Traction and Drives, in 2019. He spent a short time as a Hardware Development Engineer at Panasonic Industrial Devices Europe, Lüneburg. His research interests include SiC semiconductors and reliability in power-dense applications.

LEON FAUTH (Member, IEEE) was born in Hannover, Germany, in 1991. He received the B.Sc. and M.Sc. degrees in electrical engineering from Leibniz University Hannover, in 2018, where he is currently pursuing the Ph.D. degree in electrical engineering. Since 2018, he has also been a Research Assistant at the Institute for Drive Systems and Power Electronics, Leibniz University Hannover. His research interests include GaN power devices, high power ultrasonic applications, and hybrid topologies.

TOBIAS H. KOPP was born in Hannover, Germany, in 1985. He received the Dipl.-Ing. degree from the Technical University of Braunschweig, Germany, in 2012. Since 2013, he has been a Scientific Assistant at the Institute for High Voltage Technology and Electrical Power Systems (elenia), Technical University of Braunschweig. His current research interests include surge protective devices, vacuum interrupters, and low voltage circuit breakers.

REGINE MALLWITZ (Member, IEEE) received the Dipl.-Ing. degree in electrical engineering at the Otto-von-Guericke University Magdeburg, in 1994, and the Ph.D. degree from the University of Kassel, in 1999. She was working on pulse power problems in gas and solid lasers at Lambda Physik GmbH (currently Coherent), Göttingen, and LISA Laser Products OHG Lindau, Germany. She entered the company Eupec GmbH (currently Infineon), Warstein, as a Research and Development Engineer, in 1999, and was responsible for the development of the 1700V IGBT module family until 2004. From 2005 to 2013, she was with SMA Solar Technology AG. In 2013, she was an appointed Professor for Renewable Energies and Electromobility at the Fulda University of Applied Sciences. Since 2014, she has been a Professor of power electronics at TU Braunschweig with a strong research focus on mobility. Her special scientific interests are in the application of fast switching power semiconductors.

JENS FRIEBE (Member, IEEE) was born in Göttingen, Germany. He received the B.Sc., M.Sc., and Dr.-Ing. degree in electrical engineering from the University Kassel, Germany. He has been responsible for the research area of passive components in power electronics at the Institute for Drive Systems and Power Electronics, Leibniz University Hannover, Germany, since January 2018. Before that, he worked for more than 13 years at SMA Solar Technology, Germany, in the field of PV-inverter topologies, wide bandgap semiconductors, magnetic components, control strategies for high switching frequencies, and power electronics packaging. He invented more than 30 granted patents in the field of power electronics.

MICHAEL KURRAT (Member, IEEE) received the Dipl.-Ing. degree in electrical engineering and the Dr.-Ing. degree from the University of Dortmund, Germany, in 1988 and 1993, respectively. He previously worked at the Felten and Guilleaume Switchgear Division, Krefeld, Germany. Since 2001, he has been a Professor with the Institute for High Voltage Technology and Electrical Power Systems, elenia, Technische Universität Braunschweig, Germany, where he has been the Managing Director, since 2005. Since 2017, he has been the Dean of the Faculty of Electrical Engineering, Information Technology, Physics.

· · ·